Chronobiology International, 29(2): 103–130, (2012)

ISSN 0742-0528 print/1525-6073 online
DOI: 10.3109/07420528.2011.645707

informa
healthcare

DNA Microarray Analysis and Functional Profile of Pituitary Transcriptome Under Core-Clock Protein BMAL1 Control

F. Guillaumond,[1] D. Becquet,[2] B. Boyer,[2] O. Bosler,[2] F. Delaunay,[3] J. L. Franc,[2] and A. M. François-Bellan[2]

[1]*Aix-Marseille University, INSERM-U624, Marseille, France,* [2]*Aix-Marseille University, CRN2M, CNRS UMR 7286, Marseille, France,* [3]*IBDC, CNRS UMR 6543, Université de Nice, Nice, France*

Although it is known to contain five cell types that synthesize and release hormones with a circadian pattern, the pituitary gland is poorly characterized as a circadian oscillator. By a differential microarray analysis, 252 genes were found to be differentially expressed in pituitaries from *Bmal1*$^{-/-}$ knockout versus wild-type mice. By integrative analyses of the data set with the Annotation, Visualization, and Integrated Discovery (DAVID) Bioinformatics Resources annotation analysis system, pituitary genes with altered expression in *Bmal1*$^{-/-}$ mice were dispatched among functional categories. Clusters of genes related to signaling and rhythmic processes as well as transcription regulators, in general, were found enriched in the data set, as were pathways such as circadian rhythm, transforming growth factor β (TGFβ) signaling, valine, leucine, and isoleucine degradation, and peroxisome proliferator-activated receptor (PPAR) signaling pathways. Gene Ontology term overrepresentation analyses revealed significant enrichment for genes involved in 10 key biological processes. To determine whether genes with altered expression in *Bmal1*$^{-/-}$ mice were actually circadian genes, we further characterized in the mouse pituitary gland the daily pattern of some of these genes, including core-clock genes. Core-clock genes and genes selected from three identified overrepresented biological processes, namely, *hormone metabolic process*, *regulation of transcription from RNA polymerase II promoter*, and *cell adhesion*, displayed a rhythmic pattern. Given the enrichment in genes dedicated to cell adhesion and their daily changes in the pituitary, it is hypothesized that cell-cell interactions could be involved in the transmission of information between endocrine cells, allowing rhythmic hormone outputs to be controlled in a temporally precise manner. (Author correspondence: anne-marie.francois@univmed.fr)

Keywords: *Bmal1*$^{-/-}$ mice, Circadian rhythm, Microarray analysis, Pituitary gland

INTRODUCTION

Rhythmicity of biological functions, which is fundamental for optimal adaptation to environmental constraints, depends on coherent functioning of the so-called circadian timing system. This system is an integrated structure that operates through a hierarchy of oscillators in peripheral tissues and several brain regions, with the suprachiasmatic nucleus (SCN) of the hypothalamus functioning as the primary pacemaker or master oscillator (Duguay & Cermakian, 2009). In mammals, the SCN represents the autonomous biological clock, whereas within peripheral tissues oscillators are driven and coupled by the SCN, and they run out of phase without the driving force of the SCN, resulting in damped oscillations of peripheral organs (Reppert & Weaver, 2002; Yoo et al., 2004).

The current conception of the circadian timing system came from the observation that the genes involved in oscillatory mechanisms are contained not only in the SCN, but also in other central structures and multiple peripheral tissues and organs. The oscillatory machinery is contained within single cells expressing a network of specific clock genes that involves interacting positive and negative transcriptional feedback loops (Ko & Takahashi, 2006; Sato et al., 2006). Central to this loop are the positive elements, which include two members of the basic helix-loop-helix (bHLH)-PAS (Period-Arnt-Single-minded) transcription factor family CLOCK and BMAL1. CLOCK and BMAL1 heterodimerize and initiate transcription of target genes containing E-box *cis*-regulatory enhancer sequences, including Period (in mice, *Per1*, *Per2*, and *Per3*) and Cryptochrome (*Cry1* and *Cry2*).

Submitted July 19, 2011, Returned for revision August 25, 2011, Accepted November 24, 2011

Address correspondence to A. M. François-Bellan, Aix-Marseille University, CRN2M, CNRS UMR 6231, Faculté de Médecine Nord, Bd. Pierre Dramard CS 80011, 13344 Marseille cedex 15, France. Tel.: 33 491 698 892; Fax: 33 491 698 920; Email: anne-marie.francois@univmed.fr

Negative feedback is achieved by PER/CRY heterodimers that translocate back to the nucleus to repress their own transcription by acting on the CLOCK/BMAL1 complex (Allada et al., 2001; Sato et al., 2006). In mammals, another regulatory loop is induced by CLOCK/BMAL1 heterodimers activating transcription of two retinoic acid–related orphan nuclear receptors, *Reverbs* and *Rors* (Triqueneaux et al., 2004). REVERBs and RORs subsequently compete to bind retinoic acid–related orphan receptor response elements (ROREs) present in the *Bmal1* promoter. RORs activate transcription of *Bmal1*, whereas REVERBs repress the transcription process (Guillaumond et al., 2005; Preitner et al., 2002; Sato et al., 2006). Hence, the circadian oscillation of *Bmal1* is both positively and negatively regulated by RORs and REVERBs (Guillaumond et al., 2005). This second interlocking loop is thought to maintain the precise and robust nature of rhythms in mammals.

Most of the core circadian clock genes in the mouse exist as paralog pairs (*Per1* and *Per2*, *Cry1* and *Cry2*, *Clock* and *Npas2*), in which each gene of the pair must be knocked out to confer arrhythmicity. The only exception to this pattern is *Bmal1* (official gene name *Arntl*, also known as *Mop3*), the single knockout of which confers arrhythmicity, despite the presence of its paralog, *Bmal2* (official gene name *Arntl2*, also known as *Mop9*) (Dardente, 2008; Takahashi, 2004).

The pituitary gland is a heterogeneous organ composed of five (somatotroph, lactotroph, thyreotroph, corticotroph, and gonadotroph) cell types that secrete protein hormones (growth hormone, prolactin, thyreotrophic hormone, adrenocorticotrophic hormone, luteinizing hormone, and follicle-stimulating hormone), all with a rhythmic pattern (Haus, 2007). Although this gland constitutes the principal node of the mammalian endocrine system, its characterization as a peripheral oscillator has rarely been considered. Whereas rhythmic regulation of core-clock genes is conserved among most organs, clock-controlled genes (CCGs) are known to be tissue specific and to reflect the physiological function of a given tissue (Panda & Hogenesch, 2004). Thus, the aim of the present study was to characterize the pituitary transcriptomes that are differentially expressed in *Bmal1* knockout versus wild-type mice, and to dispatch these pituitary genes among functional categories by integrative analysis of the data set. To further determine whether genes with altered expression in *Bmal1*$^{-/-}$ mice are actually circadian genes, the daily pattern of some of them, including core-clock genes, was characterized in the mouse pituitary gland.

MATERIALS AND METHODS

Animals

Clock-deficient *Bmal1*$^{-/-}$ male mice in the C57BL/6J background (kindly provided by C. A. Bradfield, University of Wisconsin, Madison, WI, USA) were used at 8 to 12 wks of age, before they developed arthropathy (Bunger et al., 2000, 2005). Heterozygous animals were crossed to generate knockout and wild-type littermates. All animals were housed in a 12-h light/12-h dark cycle (light/dark, 12:12) with lights on at 07:00 h, in a temperature- and humidity-controlled environment and fed ad libitum. Zeitgeber time zero (ZT0) and zeitgeber time 12 (ZT12) refers to lights-on and lights-off, respectively. The light phase was provided by 36-W cool-white fluorescent tubes whose intensity level was ≈400 lux at the mid-cage level, and the dark phase by a constant dim red light (<3 lux). For DNA microarray analysis (MA), all mice were sacrificed by decapitation at ZT12 (9 mice/genotype distributed in 3 pools of 3 pituitaries). For real-time polymerase chain reaction (PCR) studies of the daily pattern of gene expression, wild-type mice (9 mice/ZT distributed in 3 pools of 3 pituitaries) were sacrificed by decapitation. Two experiments were performed with mice sacrificed either at ZT1, ZT5, ZT9, ZT13, ZT15, ZT17, ZT19, and ZT21 or at ZT2, ZT6, ZT10, ZT14, ZT18, and ZT22. Sacrifices in darkness were done under dim red light until optic nerves were sectioned. Pituitary glands taken from 3 mice from the same genotype and sacrificed at the same ZT were removed and frozen in liquid nitrogen until total RNA isolation. All experimental procedures were carried out in strict accordance with the recommendations of the European Economic Community (EEC) guidelines (86/609/EEC) for care and use of laboratory animals and met the ethical standards of the journal (Portaluppi et al., 2010).

DNA Microarrays Analysis

Pituitaries from 10-wk-old wild-type and *Bmal1*$^{-/-}$ male mice were removed at ZT12, and 3 pools of 3 pituitaries/genotype were used to isolate total RNA with a nucleospin RNA II kit (Macherey-Nagel, Hoerdt, France). RNA integrity was assessed with Agilent 2100 Bioanalyzer (Agilent Technologies, Palo Alto, CA, USA). cDNA synthesis, biotin labeling of cRNA, and hybridization on GeneChip Murine Genome 430A 2.0 arrays (Affymetrix, High Wycombe, United Kingdom) interrogating more than 14 000 substantiated mouse genes were performed in the Microarray Core Facility of the Institute of Research on Biotherapy, CHRU-INSERM-UM1 Montpellier, France (http://irb.chu-montpellier.fr/). Differentially expressed transcripts were identified using a false-discovery rate (FDR) of .1%; a minimum probe coverage of 3, an upper $\log_2$-fold change of .6, and a minimum lower $\log_2$-fold change of –.5. Fold-change was calculated as the mean from 3 pooled knockout animals/mean from 3 pooled wild-type animals.

The list of genes expressed differently in *Bmal1*$^{-/-}$ mouse pituitary was imported into the Database for Annotation, Visualization, and Integrated Discovery (DAVID) Bioinformatics Resources (http://david.abcc.ncifcrf.gov/) (Dennis et al., 2003; Huang et al., 2009a, 2009b). The David Functional Annotation Tool, which provides extended annotation coverage including over 40 databases (Sherman et al., 2007), was used to cluster

enriched annotation terms. The grouping algorithm adopts κ statistics to quantitatively measure the degree of the agreement in how genes share the similar annotation terms and fuzzy heuristic clustering to classify the groups of similar annotations according to κ values. The minimum number of annotation terms overlapped between two genes to be qualified for κ calculation was set as 3, with stringency at medium. According to DAVID recommendations, the default minimum threshold of the κ value was set to .50. Gene Ontology (GO) and Kyoto Encyclopedia of Genes and Genomes (KEGG) biological function annotations were used for DAVID analysis of enriched biological functions and pathways. The threshold of the Expression Analysis Systematic Explorer (EASE) score, a modified Fisher exact p value, for gene-enrichment analysis was set at .05 ($p \leq .05$ is considered strongly enriched in the annotation categories).

mRNA Expression Analysis

Total RNA was prepared from pituitary glands with an XS kit (Macherey-Nagel, Hoerdt, France). Total RNA (500 ng) was then used for cDNA synthesis with a high capacity RNA-to-cDNA kit (Applied Biosystem, Courtaboeuf, France), followed by real-time polymerase chain reaction (PCR) using Fast SYBR Green mix (Applied Biosystem). Expression of mRNA was normalized to the levels of the constitutively expressed *36B4* ribosomal protein mRNA levels. The sequences of the primers used in real-time PCR can be found in Supplementary Table 1.

Cosinor Analysis

Mean experimental values (± SEM), expressed as a percent of the initial value, were fitted using Prism4 software (GraphPad Software, La Jolla, CA, USA) by a nonlinear sine wave equation in which the period was constrained to 24 h: $y = \text{baseline} + \text{amplitude} \times \sin(\text{frequency} \times x + \text{phase shift})$, where $\text{frequency} = 2\pi/24$. Experimental values were considered well fitted by cosinor regression when $r^2 > .5$.

RESULTS

Genome-wide Analysis of the Pituitary Transcriptome Differentially Expressed in *Bmal1* Knockout Versus Wild-Type Mice

To investigate the pituitary transcriptome differentially expressed in *Bmal1* knockout versus wild-type mice, we

TABLE 1. Gene-term enrichment analysis by DAVID functional annotation clustering

Database	Enriched term	Enrichment score	Number of genes	% of genes	p value
GOTERM_CC_FAT	GO: 0044421 ~ extracellular region part	4.25	29	12.18	2.21E-07
SP_PIR_KEYWORDS	signal		67	28.15	6.51E-07
GOTERM_CC_FAT	GO: 0005576 ~ extracellular region		44	18.48	1.44E-06
GOTERM_CC_FAT	GO: 0005615 ~ extracellular space		21	8.82	4.54E-06
SP_PIR_KEYWORDS	biological rhythms	3.38	8	3.36	4.06E-09
GOTERM_BP_FAT	GO: 0007623 ~ circadian rhythm		8	3.36	6.52E-07
GOTERM_BP_FAT	GO: 0048511 ~ rhythmic process		11	4.62	1.04E-06
KEGG_PATHWAY	mmu04710: Circadian rhythm		6	2.52	1.23E-06
UP_SEQ_FEATURE	DNA-binding region: Basic motif	2.89	10	4.20	2.89E-04
INTERPRO	IPR001092: Basic helix-loop-helix dimerization region bHLH		8	3.36	4.52E-04
SMART	SM00353: HLH		8	3.36	6.56E-04
UP_SEQ_FEATURE	domain:Helix-loop-helix motif		8	3.36	7.83E-04
INTERPRO	IPR001628: Zinc finger, nuclear hormone receptor-type	2.67	6	2.52	2.74E-04
INTERPRO	IPR001723: Steroid hormone receptor		6	2.52	3.03E-04
INTERPRO	IPR008946: Nuclear hormone receptor, ligand-binding		6	2.52	3.34E-04
INTERPRO	IPR000536: Nuclear hormone receptor, ligand-binding, core		6	2.52	3.34E-04
UP_SEQ_FEATURE	DNA-binding region: Basic motif	2.41	10	4.2	2.89E-04
INTERPRO	IPR011700: Basic leucine zipper		4	1.68	7.54E-04
INTERPRO	IPR004827: Basic-leucine zipper (bZIP) transcription factor		5	2.1	.004390
SMART	SM00338: BRLZ		5	2.1	.005569
INTERPRO	IPR000867: Insulin-like growth factor-binding protein, IGFBP	2.38	5	2.10	7.53E-05
UP_SEQ_FEATURE	domain:IGFBP N-terminal		5	2.10	9.26E-05
SMART	SM00121: IB		5	2.10	9.75E-05
GOTERM_MF_FAT	GO: 0005520 ~ insulin-like growth factor binding		5	2.10	1.89E-04

performed a differential microarray (MA) on pituitaries from the two genotypes using DNA GeneChips. Mice were sacrificed at ZT12. ZT12 was chosen because most rhythmic transcripts yield their highest transcriptional activity at the subjective day/night transition (Oster et al., 2006). We identified 252 genes with altered expression in *Bmal1*$^{-/-}$ mice (Supplementary Table 2), comprised between 152% (upper $\log_2$ –.6-fold) and 71% (lower $\log_2$ –.5-fold) change cutoff (microarray data are available at http://www.ncbi.nlm.nih.gov/sites/GDSbrowser?acc=GSE29664). Notably, 97 of the identified target genes (38%) were up-regulated in *Bmal1*$^{-/-}$ mice, suggesting that indirect mechanisms are often involved in BMAL1-dependent transcriptional regulation (Figure 1A).

Storch et al. (2007) have shown that in the eye *Bmal1* deletion had no detectable effects on the expression of >3000 genes that are nonrhythmically expressed and was also without effect on only 10% of rhythmic genes. Thus, it may be reasonably assumed that the 252 genes with altered expression in *Bmal1*$^{-/-}$ mice in the pituitary oscillator are rhythmic and, therefore, may be defined as CCGs. However, when comparing our data set with the pituitary circadian transcriptome previously published (Hughes et al., 2010), only 53 genes out of 343 from this list were found to be included in our data set (Figure 1B and Supplementary Table 3). Conversely, 199 genes from our data set were not previously identified as rhythmic genes by Hughes et al. (2010) (Figure 1B and Supplementary Table 3). This only partial overlap thus pointed out the obvious discrepancies, revealing the influence of different criteria and assay stringency for a gene to be considered as CCGs between circadian studies (Duffield, 2003).

To compare our list of pituitary genes with altered expression in *Bmal1*$^{-/-}$ mice with CCGs identified in another well-characterized oscillator, the liver, we, therefore, merged data sets from several studies performed on the liver (Miller et al., 2007; Panda et al., 2002; Storch et al., 2002; Ueda et al., 2002), as previously reported (Guillaumond et al., 2010). This comparative analysis indicated <15% of CCGs were common between the liver and pituitary (Figure 1C). Of note, if we merged our data set with that of Hughes et al. (2010) to obtain a more complete list of pituitary CCGs, the comparative analysis between pituitary and hepatic CCGs gave similar results, since in this case we found <10% of CCGs were common between these two tissues (data not shown). These results confirm that CCGs are tissue specific and reflect the physiological function of a given tissue (Delaunay & Laudet, 2002; Panda & Hogenesch, 2004; Panda et al., 2002). Transcripts that cycle in several tissues may then represent basic circadian outputs of cellular physiology or components of the circadian oscillator, itself. Actually, core-clock genes represented almost a quarter of genes that merged between pituitary and hepatic circadian transcriptomes (data not shown).

We next compared our list of 252 genes with altered expression in *Bmal1*$^{-/-}$ mice with a list of genes identified by chromatin immunoprecipitation (ChIP) as direct BMAL1 target genes in the liver (1574-gene data set from Rey et al. [2011]). This comparison indicated that 29 genes of our data set are direct BMAL1 target genes in the liver (Figure 1C). Among these 29 genes, 8 were core-clock genes and 14 were included in the 31-gene list common to the data set of rhythmically expressed genes in the liver and genes with altered expression in *Bmal1*$^{-/-}$ mouse pituitary; of note, 7 of these 14 genes were core-clock genes (Figure 1C). The fact that only 11% of the genes with altered expression in *Bmal1*$^{-/-}$ mouse pituitary were included in the list of genes that harbor BMAL1 binding sites, as determined by chromatin immunoprecipitation using BMAL1 antibodies in the liver (Rey et al., 2011), is in line with the conception that only a few CCGs are under the direct control of the circadian clock. Further, the proportion of potential direct BMAL1 targets within the circadian hepatic transcriptomes was of the same order, since only 10% of hepatic CCGs were included in the list of genes that harbor BMAL1 binding sites (data not shown). This clearly reinforces the notion that a large part, if not most, of the transcriptional regulation of mammalian clock outputs is indirect, as suggested by the early work on Drosophila (McDonald & Rosbash, 2001).

Biological Pathways and Functions Subjected to BMAL1 Regulation

Our data set of 252 genes was analyzed with the DAVID Bioinformatics Resources. DAVID provides a clustering function that forms sets of overlapping gene categories. Functional annotation analysis with DAVID identified 10 annotation clusters with an enrichment score >1.5 (Supplementary Table 4). The most prominent enriched annotation clusters related to signaling, rhythmic process, and transcription regulators, in general, including zinc finger, basic helix-loop-helix factors, nuclear hormone receptor, and basic leucine zipper (DAVID, $p < .05$); the four most significant annotation categories found for the six most prominent clusters are given in Table 1. Analysis of the differentially expressed genes by the KEGG pathways classification showed that circadian rhythm, transforming growth factor β (TGFβ) signaling, valine, leucine, and isoleucine degradation, and peroxisome proliferator-activated receptor (PPAR) signaling pathways were significantly enriched in our data set (DAVID, $p < .05$; Table 2). Genes from these different signaling pathways that were found differentially expressed in *Bmal1*$^{-/-}$ mouse pituitary are indicated in Supplementary Figure 1. We next dispatched genes with altered expression in *Bmal1*$^{-/-}$ mouse pituitary among functional categories using the controlled vocabulary of the Gene Ontology Consortium. This statistical analysis of the biological processes represented in

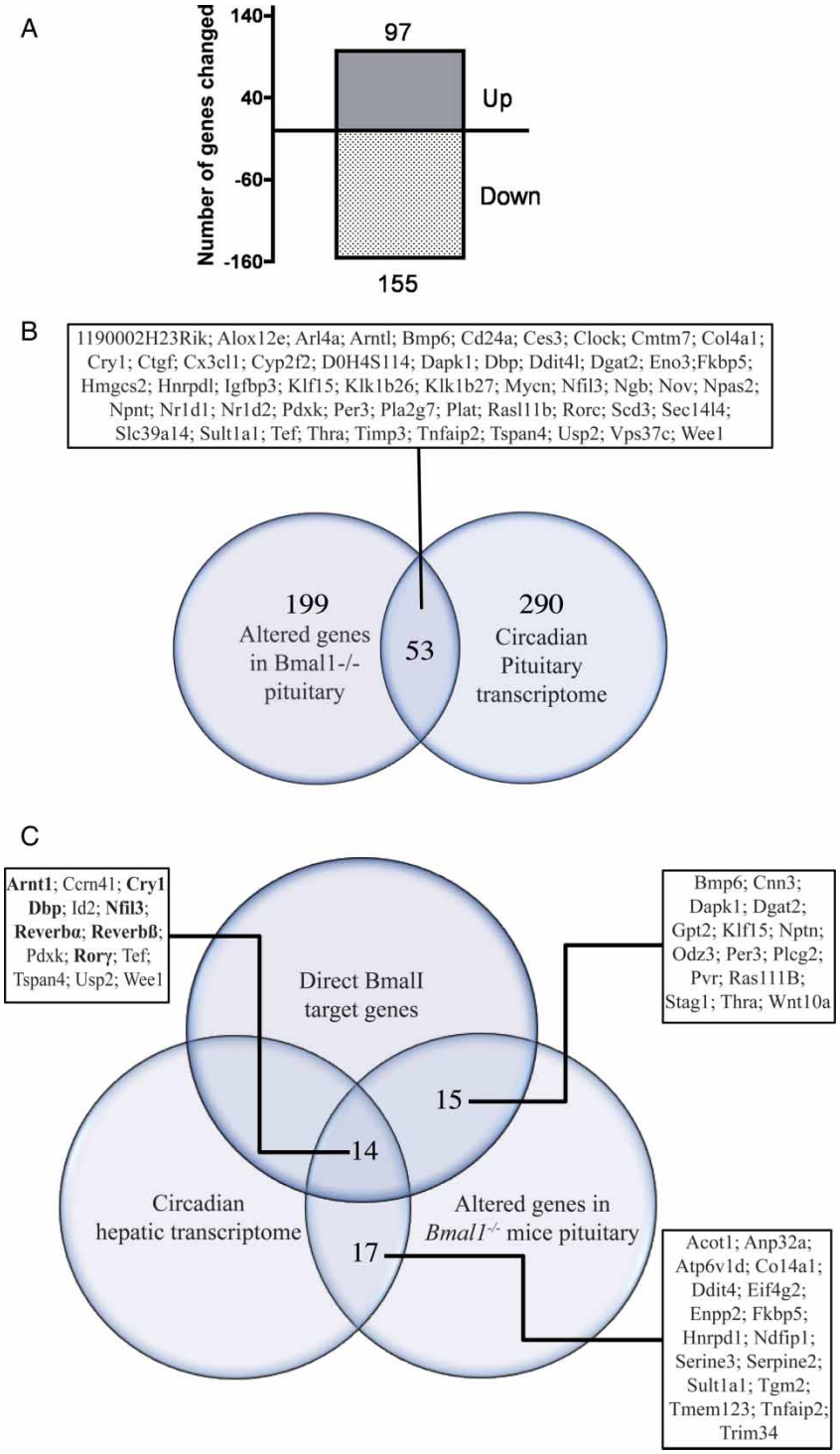

FIGURE 1. Genome-wide comparison of ZT12 pituitary mRNA profiles from wild-type and *Bmal1*$^{-/-}$ male mice. (A) Total number of genes up- or down-regulated in *Bmal1*$^{-/-}$ mouse pituitary. (B) Overlap between genes with altered expression in *Bmal1*$^{-/-}$ mouse pituitary and circadian pituitary transcriptome published previously (Hughes et al., 2010). (C) Overlap between genes with altered expression in *Bmal1*$^{-/-}$ mouse pituitary, circadian hepatic transcriptomes published previously (data sets used were from Miller et al. [2007], Panda et al. [2002], Storch et al. [2002], and Ueda et al. [2002]), and direct BMAL1-target genes published previously in the liver (data set from Rey et al. [2011]). Core-clock genes are shown in bold.

our data set revealed a significant enrichment for genes involved in 10 key biological processes, namely, *rhythmic process*, *regulation of cell growth*, *hormone metabolic process*, *response to hormone stimulus*, *lipid metabolic process*, *positive regulation of RNA metabolic process*, *cell adhesion*, *regulation of cell death*, *regulation of transcription from RNA polymerase II promoter*, and *system development* (Table 3). Each of these

TABLE 2. List of the pathways identified by the KEGG Classification System analysis for the 252 significantly altered genes in *Bmal1* knockdown pituitary glands

Term	Genes	%	*p* value
Circadian rhythm	*Arntl*; *Clock*; *Npas2*; *Nr1d1*; *Per3*; *Cry1*	2.5	1.20E-06
TGFβ signaling	*Bmp6*; *Dcn*; *Id1*; *Id2*; *Id4*; *Cdkn2b*	2.5	1.40E-02
Valine, leucine, and isoleucine degradation	*Hmgcs2*; *Oxct1*; *Aldh6a1*; *Bcat1*	1.7	3.90E-02
PPAR signaling	*Hmgcs2*; *Acsl6*; *Fabp7*; *Me1*; *Scd3*	2.1	4.00E-02

TABLE 3. Biological processes associated with genes whose expression was altered in *Bmal1*$^{-/-}$ mouse pituitary as determined by Gene Ontology-term enrichment

GO ID	Term	Modified genes	*p* value	Fold enrichment	Genes
GO:0048511	Rhythmic process	11	1.056E-06	8.020	*Ccrn4l*, *Arntl*, *Npas2*, *Nr1d1*, *Dbp*, *Tef*, *Per3*, *Nfil3*, *Cry1*, *Ncor1*, *Clock*
GO:0001558	Regulation of cell growth	6	.0092	4.66	*Nov*, *Wisp1*, *Ctgf*, *Mapt*, *Esm1*, *Igfbp3*
GO:0042445	Hormone metabolic process	5	.0369	3.97	*Aldhia2*, *Rbp4*, *Dio2*, *Adh7*, *Nr3c1*
GO:0009725	Response to hormone stimulus	7	.0279	3.031	*Me1*, *Rbp4*, *Hmgcs2*, *LOC677317*, *Mgp*, *Gal*, *Timp3*, *Cd24a*
GO:0006629	Lipid metabolic process	23	.0002	2.361	*Pgap2*, *Rbp4*, *Scd3*, *Pik3c2a*, *Alox12e*, *Enpp2*, *Ugt8a*, *Sorl1*, *Acot1*, *Adh7*, *Nr3c1*, *Pip5k1a*, *Gdp3*, *Aldh1a2*, *Dgat2*, *Hmgcs2*, *Smpdl3a*, *Sult1a1*, *LOC100047936*, *Plcg2*, *Mboat1*, *Pla2g7*, *Hsd11b1*, *Acsl6*
GO:0051254	Positive regulation of RNA metabolic process	13	.0144	2.217	*Eny2*, *Cebpb*, *Thra*, *Nr4a2*, *Sox4*, *Klf15*, *Arntl*, *Plagl1*, *Npas2*, *Tef*, *Neurod1*, *Jak3*, *Clock*
GO:0007155	Cell adhesion	16	.0119	2.038	*Pvr*, *Thra*, *Ptprm*, *Npnt*, *Cpxm2*, *Edil3*, *Neo1*, *Cx3cl1*, *Cd24a*, *Mia1*, *Wisp1*, *Col7a1*, *Ctgf*, *Nptn*, *Cntn1*, *Spp1*
GO:0010941	Regulation of cell death	15	.0260	1.904	*Pgap2*, *Cebpb*, *Nr4a2*, *Nr3c1*, *Pea15a*, *Cx3cl1*, *Gal*, *Cd24a*, *Dapk1*, *Serinc3*, *Plcg2*, *Tgm2*, *Neurod1*, *Igfbp3*, *Spp1*
GO:0006357	Regulation of transcription from RNA polymerase II promoter	16	.0254	1.856	*Cebpb*, *Thra*, *Trim27*, *Nr4a2*, *Sox4*, *Arntl*, *Plagl1*, *Npas2*, *Id2*, *Id1*, *Tef*, *Neurod1*, *Jak3*, *Per3*, *Ncor1*, *Clock*
GO:0048731	System development	44	.0027	1.551	*Rbp4*, *Insl3*, *Thra*, *Npnt*, *Sox4*, *Rorc*, *Cx3cl1*, *Elk3*, *Nr3c1*, *Grem1*, *Cd24a*, *Timp3*, *Ckb*, *Aldh1a2*, *Ank1*, *Serpine2*, *Ctgf*, *Mapt*, *Tgm2*, *Tgfa*, *Acsl6*, *Spp1*, *Wnt10a*, *Cebpb*, *Ugt8a*, *Nr4a2*, *Mgp*, *Gal*, *Ywhae*, *Mycn*, *Id2*, *Id1*, *Plcg2*, *Nptn*, *Hsd11b1*, *Ush1c*, *Neurod1*, *Id4*, *Jak3*, *Fabp7*, *Igfbp3*, *Tnfaip2*, *Ncor1*, *Bmp6*

functional clusters displayed an enrichment score >1.5-fold and contained 5 to 44 genes with altered expression in *Bmal1*$^{-/-}$ mouse pituitary.

Daily Pattern of Core-Clock Gene Expression in the Mouse Pituitary

As expected, most core-clock genes in the pituitary were found affected by *Bmal1* deletion in DNA microarray analysis. We selected some of these genes, namely *Clock*, *Npas2*, *Rorγ*, and *Reverbα* (official gene name *Nr1d1*) to validate the microarray data by quantitative PCR (qPCR). Microarrays and qPCR gave highly consistent results, although the amplitude of the BMAL1 regulation always appeared underestimated in microarray analysis (Figure 2A).

We next characterized in the pituitary gland the daily pattern of core-clock genes mentioned above and that of *Bmal1*, itself, in wild-type mice sacrificed at different ZT (3 pools of 3 pituitaries/time point). As shown in Figure 2B, *Bmal1* mRNA levels displayed a rhythmic pattern in mouse pituitary glands over the 24-h light/dark cycle; they were fitted by the following equation: $y = .775 - .468 \times \sin\ (.26x - 19.92)$, with an $r^2 = .875$ (Figure 2B). Levels gradually decreased across the light phase, reaching a nadir at the transition between the light and dark phases (Figure 2B). Then, levels increased during the dark phase, reaching an acrophase (peak time) at ZT21 (Figure 2B). *Clock* mRNA levels, which fluctuated slightly in low amplitude over the 24-h light/dark cycle, were fitted by the following equation: $y = 1.059 - .211 \times \sin\ (.26x + .503)$, with $r^2 = .777$ (Figure 2B). *Npas2* mRNA levels significantly varied with time and were fitted by the following equation: $y = .496 + .406 \times \sin\ (.26x + .109)$, with

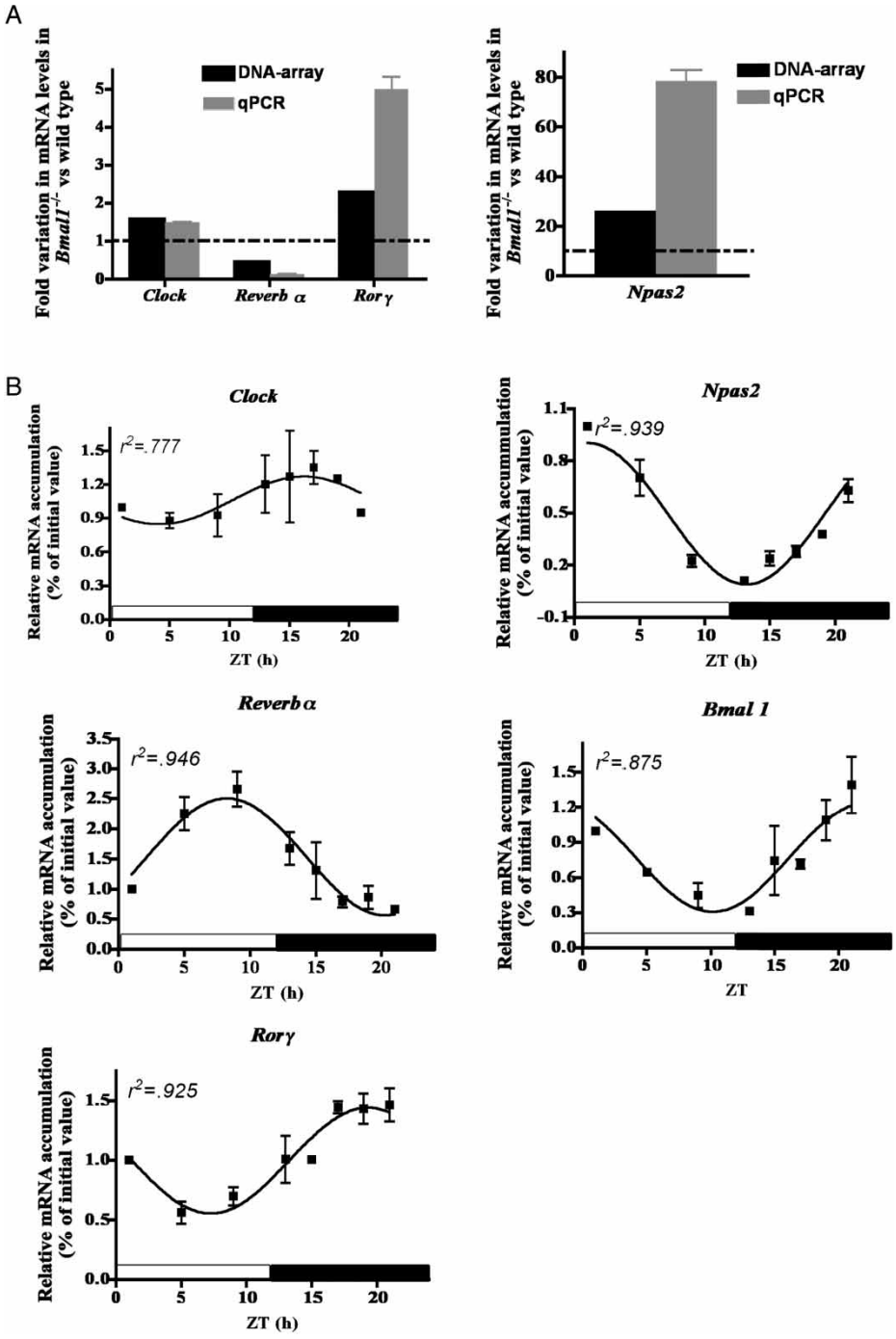

FIGURE 2. (A) Comparison of the amplitude of BMAL1 regulation of core-clock genes by MA and qPCR analysis. (B) Daily pattern of expression of five main core-clock genes in the pituitary of mice maintained in a 12-h/12-h light-dark cycle. Total RNA was prepared from pituitary glands taken from 3 wild-type mice sacrificed at the same ZT and then used for cDNA synthesis followed by real-time PCR analysis. White and black bars designate the light and dark phases, respectively. Results, expressed as a percent of initial value, are mean ± SEM and are fitted with a cosinor curve. $r^2 > .5$ is considered significant.

$r^2 = .939$. As described for the *Bmal1* mRNA rhythmic pattern, *Npas2* mRNA levels gradually decreased across the light phase, reaching a nadir at the transition between the light and dark phases, and then increased during the dark phase (Figure 2B). *Rorγ* mRNA levels displayed a rhythmic pattern and were fitted by the following equation: $y = .999 - .444 \times \sin(.26x + .131)$, with $r^2 = .925$. *Rorγ* mRNA levels displayed a nadir in the mid-light phase and highest levels in the second half of the dark phase (Figure 2B). As previously shown in other structures, the rhythmic pattern of *Reverbα* mRNA was antiphasic to that of *Bmal1*, *Npas2*, and *Rorγ* (Figure 2B). Levels of mRNA were fitted by the following equation: $y = 1.53 + .971 \times \sin(.26x - .564)$, with $r^2 = .946$. They were high during the light phase, with an acrophase ~ZT10, and then declined to reach their lowest values during the dark phase (Figure 2B).

Daily Pattern of Genes With Altered Expression in *Bmal1*$^{-/-}$ Mouse Pituitary

To determine whether some genes with altered expression in *Bmal1*$^{-/-}$ mice identified in the MA were actually circadian genes, we selected five genes that were classified in either *hormone metabolic process* (*Dio2* and *Rbp4*), *regulation of transcription (Tef*), or *cell adhesion* (*Cd24a* and *Cntn1*) (Table 3) and determined whether they displayed a daily pattern of expression in the pituitary gland. First, we verified that microarrays and qPCR gave consistent results, relative to BMAL1 regulation (Figure 3A).

Although two of these five selected genes, namely, *Tef* and *Cd24a*, were previously identified as CCGs in the pituitary, this was not the case for the three others, *Dio2*, *Rbp4*, and *Cntn1* (Hughes et al., 2010). However,

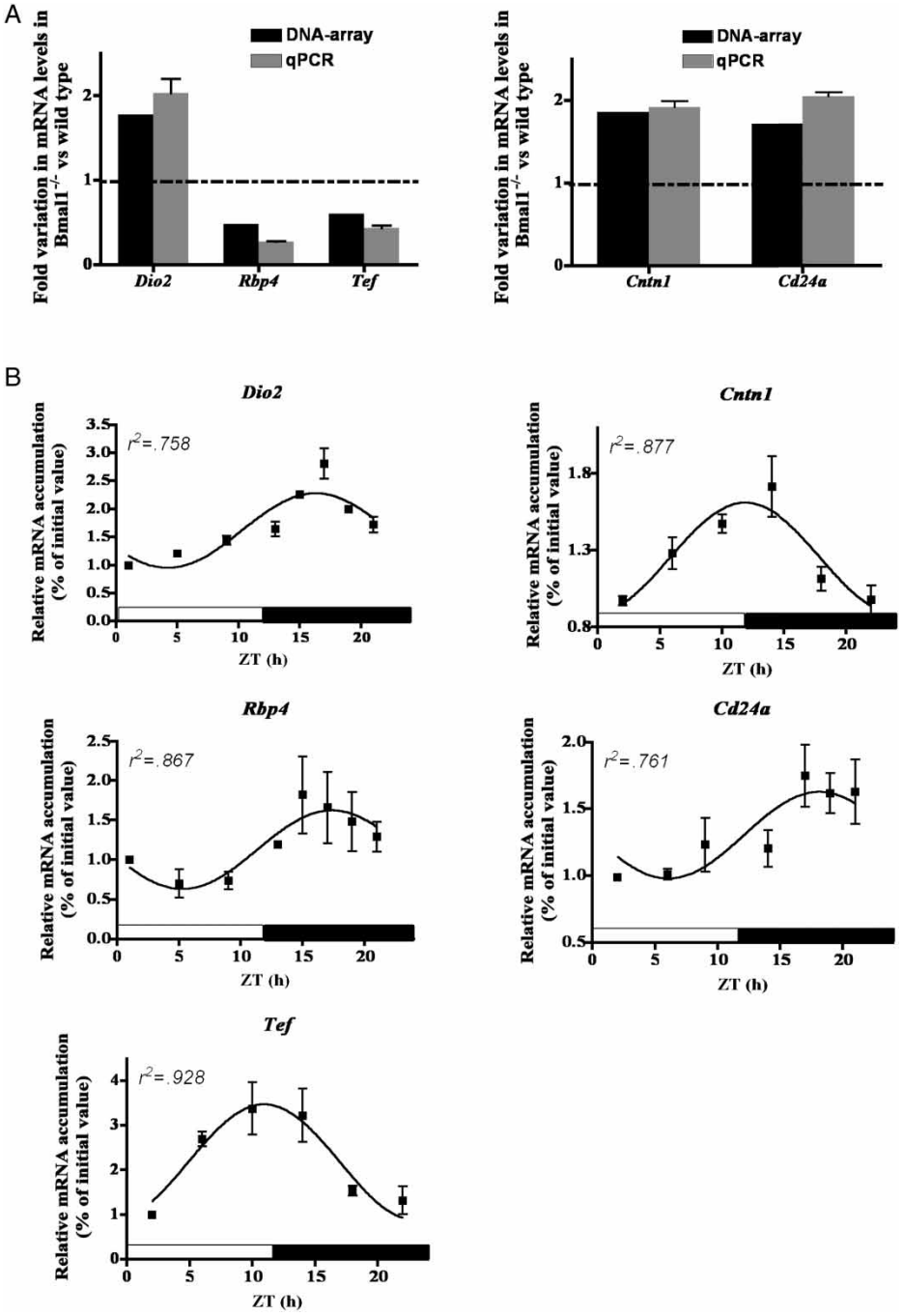

FIGURE 3. (A) Comparison of the amplitude of BMAL1 regulation of five BMAL1-regulated genes by MA and qPCR analysis. (B) Daily pattern of expression of five BMAL1-regulated genes in the pituitary of mice maintained in a 12-h/12-h light-dark cycle. Total RNA was prepared from pituitary glands taken from 3 wild-type mice sacrificed at the same ZT and then used for cDNA synthesis followed by real-time PCR analysis. White and black bars designate the light and dark phases, respectively. Results, expressed as a percent of initial value, are mean ± SEM and are fitted with a cosinor curve. $r^2 > .5$ is considered significant.

we found here that all five selected genes displayed a daily pattern of expression as determined by qPCR. Levels of *Cd24a* mRNA, *Dio2* mRNA, and *Rbp4* mRNA were fitted by the following equations, respectively: $y = .117 + .164 \times \sin(.26x + .579)$, with $r^2 = .761$; $y = .126 + .168 \times \sin(.26x + .274)$, with $r^2 = .758$; $y = 1.12 - .495 \times \sin(.26x + .201)$, with $r^2 = .867$ (Figure 3B). Levels of *Cd24a*, *Dio2*, and *Rbp4* mRNAs attained their acrophase in the mid-dark period (Figure 3B). *Cntn1* and *Tef* mRNA levels increased earlier, reaching maximal levels at around the transition between the light and dark phases (Figure 3B). They were fitted by the following equations, respectively: $y = 1.25 + .357 \times \sin(.26x - 7.79)$, with $r^2 = .877$; $y = 2.17 + 1.29 \times \sin(.26x - 1.27)$, with $r^2 = .928$ (Figure 3B).

DISCUSSION

The transcriptional networks relaying time information from the circadian clock to physiological processes were characterized here in the pituitary gland using mice deleted in *Bmal1* gene, the only single knockout core-clock gene that confers arrhythmicity (Dardente, 2008; Takahashi, 2004).

Two hundred and fifty-two genes were found to be differentially expressed in the pituitary gland from *Bmal1* knockout compared to wild-type mice. Although it cannot be determined which of these 252 genes are driven by BMAL1 locally in the pituitary and which are being driven by a nonpituitary oscillator, in particular the SCN, it was striking that these 252 genes represented ~4% of the genes found expressed in the pituitary gland, a percentage that is consistent with that (1–10%) found in other studies in which the circadian transcriptome was examined in different tissues (Delaunay & Laudet, 2002). However, since the overlap between our data set and the previously reported pituitary circadian transcriptome (Hughes et al., 2007, 2010) was only partial, the proportion of CCGs in the pituitary is probably higher.

Our KEGG classification system analysis identified important pathways that have been previously linked to circadian function, such as TGFβ and PPAR signaling (Rey et al., 2011). A GO-based statistical analysis of the biological processes represented in our data set revealed a significant enrichment for genes controlling biological process, such as *rhythmic process*, *regulation of cell growth*, *hormone metabolic process*, *response to hormone stimulus*, *lipid metabolic process*, *positive regulation of RNA metabolic process*, *cell adhesion*, *regulation of cell death*, *regulation of transcription from RNA polymerase II promoter*, and *system development*. Genes annotated with GO terms and involved in the control of these different biological processes represented between 4.5% (for rhythmic process) to 17% (for system development) of the genes with altered expression in *Bmal1*$^{-/-}$ mouse pituitary. The high proportion of genes involved in developmental and metabolic processes was consistent with the significant effects of the knockout of *Bmal1* on longevity and metabolism (Bunger et al., 2005). Not less than 16 genes were found involved in transcription, suggesting that in the pituitary, as in other tissues, transcription factors may constitute molecular links between circadian clock and physiological outputs.

Among genes with altered expression in *Bmal1*$^{-/-}$ mouse pituitary, 11 genes were classified in rhythmic process. Note that among the *Per* paralog genes (*Per1*, *Per2*, and *Per3*), only *Per3* was found included in the set of genes with altered expression in *Bmal1*$^{-/-}$ mouse pituitary with the stringent cutoff used in our analysis; but when using a less stringent cutoff, both *Per1* and *Per2* were shown to be down-regulated in *Bmal1*$^{-/-}$ mouse pituitary. Nevertheless, we kept stringent conditions to prevent the inclusion of false positives in our data set. All core-clock genes were expressed in the pituitary, and we characterized the rhythmic expression of some of them. Our results are not only consistent with those obtained in a global rhythmic MA performed in the pituitary (Hughes et al., 2007, 2010) but also extend those recently reported by Bur et al. (2010). As expected, core-clock genes displayed marked amplitude of expression along the daily cycle, with the exception of *Clock* transcription that failed to do so, as also reported by Bur et al. (2010). As previously reported (Bur et al., 2010; Hughes et al., 2007, 2010), we found *Bmal1* and *Npas2* to display the lowest mRNA levels at the day/night transition. Consistent with their respective negative and positive regulation of *Bmal1*, *Reverbα* and, *Rorγ* displayed a pattern of mRNA expression antiphasic or in phase with that of *Bmal1*, respectively. By showing the daily expression of most core-clock genes with transcription phase angles similar to those in other circadian oscillators (Reppert & Weaver, 2002), our results, together with those previously published (Bur et al., 2010; Hughes et al., 2007, 2010), support the idea that the pituitary gland houses a circadian clock.

A few genes from functional categories, such as *hormone metabolic process*, *regulation of transcription from RNA polymerase II promoter*, and *cell adhesion*, were further selected with the double objective to validate the microarray data by qPCR and to study their potential rhythmic pattern in the pituitary. Although the amplitude of the BMAL1 regulation always appeared weaker in MA, the qPCR analysis in all cases validated results obtained by MA. Moreover, in line with a study showing in the eye that 90% of genes with altered expression in *Bmal1*$^{-/-}$ mice are CCGs (Storch et al., 2007), the expression of all selected genes followed a rhythmic daily pattern. Although some of these selected genes (*Tef* and *Cd24a*) were previously identified as CCGs in the pituitary, this was not the case for the others (*Dio2*, *Rbp4*, and *Cntn1)* (Hughes et al., 2007, 2010). Then, our data set of genes with altered expression in

Bmal1$^{-/-}$ mice provided additional information on the pituitary circadian transcriptome.

Among the genes we selected to study their potential rhythmic pattern of expression, *Dio2*, an enzyme responsible for the conversion of thyroxine (T4) to triiodothyronine (T3), is an important regulator of the local concentration of intracellular T3 (Bianco et al., 2002; Gereben & Salvatore, 2005). As in the rat pineal gland, where its activity is rhythmic, increasing during the hours of darkness (Guerrero & Reiter, 1992; Murakami et al., 1989; Tanaka et al., 1987), we showed here that *Dio2*, identified in MA as a gene with altered expression in *Bmal1*$^{-/-}$ mice, displayed a daily rhythmic pattern of expression in the pituitary gland. This was also the case for *Rbp4*. RBP4 belongs to the lipocalin family and is a specific carrier for retinol (vitamin A) in the blood. RBP4, previously thought to play a role only in the delivery of retinol from the liver to peripheral tissues, has been classified now as a novel adipokine implicated in the pathophysiology of insulin resistance (Yang et al., 2005). Although its roles in the pituitary and the pituitary cell types that express this protein are unknown, it is interesting that *Rbp4* was shown here to be a gene with altered expression in *Bmal1*$^{-/-}$ mice displaying rhythmic expression in the pituitary, given the increasing evidence that obesity, metabolic syndrome, and insulin resistance are highly correlated with the expressions of core-clock genes and their downstream, circadian CCGs (Bass & Takahashi, 2010). A daily rhythm in the expression of the PAR-bZIP family member, thyrotroph embryonic factor (*Tef*), considered as an important output of the circadian clock (Fonjallaz et al., 1996), was also found here in the pituitary gland. This transcriptional factor was recently shown to control the expression of the thyrotrophin β subunit RNA (*Tshβ*) in the pars tuberalis of the pituitary gland and to be involved in the molecular pathway linking the circadian clock to seasonal timing in mammals (Dardente et al., 2010).

A very interesting group of genes emerging from the DAVID analysis was that of cell adhesion. It has been previously shown that genes involved in cell-adhesion processes are also enriched in the rhythmic transcriptome of another endocrine tissue, the pineal gland (Bustos et al., 2011). Endocrine cells in the mammalian pituitary are arranged into three-dimensional networks that wire the gland and act to optimize rhythmic hormone output by allowing the transmission of information between cell ensembles in a temporally precise manner (Hodson et al., 2010). In this respect, it was interesting that 16 genes with altered expression in *Bmal1*$^{-/-}$ mouse pituitary were classified into cell-adhesion processes that could be involved in the organization of these networks. Among them, CD24, also known as nectadrin (Fischer et al., 1990), is a glycosylphosphatidylinositol-anchored adhesion molecule that is expressed in hematopoietic and neural cells. Although the function of CD24 has not been clearly demonstrated, to date, CD24 has been implicated in the control of cell-cell and cell-substrate binding as well as in cell signaling (Sammar et al., 1997). When presented on transfected cells as a monolayer substratum, CD24 inhibits neurite outgrowth and branching of the peripheral nervous system and central nervous system (CNS) neurons (Shewan et al., 1996). This gene displays a rhythmic pattern of expression in the rat pineal gland, with a peak level at the end of the dark phase (Smith et al., 2001). Thus, it was of particular interest to observe here that *Cd24* appeared as a rhythmically regulated gene in another endocrine tissue, the pituitary gland, even if its peak level in this tissue (mid-dark phase) differed from that in the pineal gland (Smith et al., 2001). In addition, the gene encoding another glycosylphosphatidylinositol-anchored cell-adhesion molecule of the immunoglobulin superfamily, *Cntn1*, also displayed a rhythmic pattern of expression in the pituitary gland. Cell-adhesion molecules are believed to play a crucial role in the circadian system. For instance, polysialic acid (PSA) is a carbohydrate polymer attached to neural cell-adhesion molecule (NCAM). PSA-NCAM exhibits a striking daily rhythm of expression in the SCN and is believed necessary for creating appropriate cell-surface reorganizations that are intrinsic to the master clock-resetting mechanism (Girardet et al., 2010; Glass et al., 2003). More recently, expression of E-cadherin and claudin-4 has been reported to follow a circadian rhythm in the kidney, and the dynamic change in these protein levels has been implicated in the level of sodium excretion (Yamato et al., 2010). The daily changes in genes dedicated to cellular interactions and extracellular matrix biology provide clear evidence of the dynamic nature of these processes. This might impact the tightness of junctions between cells and the ability of circulating compounds and cells to gain access to the surface of pituitary cells. Future investigations should explore whether the daily pattern in *Cd24a* and *Cntn1* we report here in the pituitary gland could be involved in the transmission of information between the endocrine cells, allowing rhythmic hormone outputs to be controlled in a temporally precise manner.

Although the present study together with previous ones (Bur et al., 2010; Hughes et al., 2007, 2010) support the idea that the pituitary gland houses a circadian clock, the importance of the intrinsic clock in pituitary physiology remains to be evaluated. By providing evidence that in a rat sommatolactotroph cell line prolactin-gene expression displayed a rhythmic pattern (Guillaumond et al., 2011), we recently showed that the intrinsic clock in adenohypophyseal cells, at least sommatolactotrophs, contributes to the generation of hormonal rhythms in the pituitary gland. Further works are currently in progress to reconsider the pituitary for its role as an autonomous generator of circadian rhythmicity, and not solely as a structure that would be only slaved to hypothalamic neuropeptide control.

ACKNOWLEDGMENTS

The authors thank Gary Burkhart for editing.

Declaration of Interest: The authors report no conflicts of interest. The authors alone are responsible for the content and writing of the paper.

REFERENCES

Allada R, Emery P, Takahashi JS, Rosbash M. (2001). Stopping time: the genetics of fly and mouse circadian clocks. *Annu. Rev. Neurosci.* 24:1091–1119.

Bass J, Takahashi JS. (2010). Circadian integration of metabolism and energetics. *Science* 330:1349–1354.

Bianco AC, Salvatore D, Gereben B, Berry MJ, Larsen PR. (2002). Biochemistry, cellular and molecular biology, and physiological roles of the iodothyronine selenodeiodinases. *Endocr. Rev.* 23:38–89.

Bunger MK, Wilsbacher LD, Moran SM, Clendenin C, Radcliffe LA, Hogenesch JB, Simon MC, Takahashi JS, Bradfield CA. (2000). Mop3 is an essential component of the master circadian pacemaker in mammals. *Cell* 103:1009–1017.

Bunger MK, Walisser JA, Sullivan R, Manley PA, Moran SM, Kalscheur VL, Colman RJ, Bradfield CA. (2005). Progressive arthropathy in mice with a targeted disruption of the Mop3/Bmal-1 locus. *Genesis* 41:122–132.

Bur IM, Zouaoui S, Fontanaud P, Coutry N, Molino F, Martin AO, Mollard P, Bonnefont X. (2010). The comparison between circadian oscillators in mouse liver and pituitary gland reveals different integration of feeding and light schedules. *PLoS ONE* 5:pe15316.

Bustos DM, Bailey MJ, Sugden D, Carter DA, Rath MF, Møller M, Coon SL, Weller JL, Klein DC. (2011). Global daily dynamics of the pineal transcriptome. *Cell Tissue Res.* 344:1–11.

Dardente H. (2008). [Synchronization and genetic redundancy in circadian clocks]. *Med. Sci. (Paris)* 24:270–276.

Dardente H, Wyse CA, Birnie MJ, Dupré SM, Loudon AS, Lincoln GA, Hazlerigg DG. (2010). A molecular switch for photoperiod responsiveness in mammals. *Curr. Biol.* 20:2193–2198.

Delaunay F, Laudet V. (2002). Circadian clock and microarrays: mammalian genome gets rhythm. *Trends Genet.* 18:595–597.

Dennis G, Sherman BT, Hosack DA, Yang J, Gao W, Lane HC, Lempicki RA. (2003). DAVID: Database for Annotation, Visualization, and Integrated Discovery. *Genome Biol.* 4:P3.

Duguay D, Cermakian N. (2009). The crosstalk between physiology and circadian clock proteins. *Chronobiol. Int.* 26:1479–1513.

Fischer GF, Majdic O, Gadd S, Knapp W. (1990). Signal transduction in lymphocytic and myeloid cells via CD24, a new member of phosphoinositol-anchored membrane molecules. *J. Immunol.* 144:638–641.

Fonjallaz P, Ossipow V, Wanner G, Schibler U. (1996). The two PAR leucine zipper proteins, TEF and DBP, display similar circadian and tissue-specific expression, but have different target promoter preferences. *EMBO J.* 15:351–362.

Gereben B, Salvatore D. (2005). Pretranslational regulation of type 2 deiodinase. *Thyroid* 15:855–864.

Girardet C, Becquet D, Blanchard MP, François-Bellan AM, Bosler O. (2010). Neuroglial and synaptic rearrangements associated with photic entrainment of the circadian clock in the suprachiasmatic nucleus. *Eur. J. Neurosci.* 32:2133–2142.

Glass JD, Watanabe M, Fedorkova L, Shen H, Ungers G, Rutishauser U. (2003). Dynamic regulation of polysialylated neural cell adhesion molecule in the suprachiasmatic nucleus. *Neuroscience* 117:203–211.

Guerrero JM, Reiter RJ. (1992). Iodothyronine 5′-deiodinating activity in the pineal gland. *Int. J. Biochem.* 24:1513–1523.

Guillaumond F, Dardente H, Giguère V, Cermakian N. (2005). Differential control of Bmal1 circadian transcription by REV-ERB and ROR nuclear receptors. *J. Biol. Rhythms* 20:391–403.

Guillaumond F, Gréchez-Cassiau A, Subramaniam M, Brangolo S, Peteri-Brünback B, Staels B, Fiévet C, Spelsberg TC, Delaunay F, Teboul M. (2010). Kruppel-like factor KLF10 is a link between the circadian clock and metabolism in liver. *Mol. Cell Biol.* 30:3059–3070.

Guillaumond F, Boyer B, Becquet D, Guillen S, Kuhn L, Garin J, Belghazi M, Bosler O, Franc JL, François-Bellan AM. (2011). Chromatin remodeling as a mechanism for circadian prolactin transcription: rhythmic NONO and SFPQ recruitment to HLTF. *FASEB J.* 25:2740–2756.

Haus E. (2007). Chronobiology in the endocrine system. *Adv. Drug Deliv. Rev.* 59:985–1014.

Hodson DJ, Molino F, Fontanaud P, Bonnefont X, Mollard P. (2010). Investigating and modelling pituitary endocrine network function. *J. Neuroendocrinol.* 22:1217–1225.

Huang da W, Sherman BT, Lempicki RA. (2009a). Bioinformatics enrichment tools: paths toward the comprehensive functional analysis of large gene lists. *Nucleic Acids Res.* 37:1–13.

Huang da W, Sherman BT, Lempicki RA. (2009b). Systematic and integrative analysis of large gene lists using DAVID bioinformatics resources. *Nat. Protocols* 4:44–57.

Hughes M, Deharo L, Pulivarthy SR, Gu J, Hayes K, Panda S, Hogenesch JB. (2007). High-resolution time course analysis of gene expression from pituitary. *Cold Spring Harb. Symp. Quant. Biol.* 72:381–386.

Hughes ME, Hogenesch JB, Kornacker K (2010). JTK_CYCLE: an efficient nonparametric algorithm for detecting rhythmic components in genome-scale data sets. *J. Biol. Rhythms* 25:372–380.

Ko CH, Takahashi JS. (2006). Molecular components of the mammalian circadian clock. *Hum. Mol. Genet.* 15(Spec. No. 2):R271–R277.

McDonald MJ, Rosbash M. (2001). Microarray analysis and organization of circadian gene expression in *Drosophila*. *Cell* 107:567–578.

Miller BH, McDearmon EL, Panda S, Hayes KR, Zhang J, Andrews JL, Antoch MP, Walker JR, Esser KA, Hogenesch JB, Takahashi JS. (2007). Circadian and CLOCK-controlled regulation of the mouse transcriptome and cell proliferation. *Proc. Natl. Acad. Sci. U. S. A.* 104:3342–3347.

Murakami M, Greer MA, Greer SE, Hjulstad S, Tanaka K. (1989). Comparison of the nocturnal temporal profiles of *N*-acetyl-transferase and thyroxine 5′-deiodinase in rat pineal. *Neuroendocrinology* 50:88–92.

Oster H, Damerow S, Hut RA, Eichele G. (2006). Transcriptional profiling in the adrenal gland reveals circadian regulation of hormone biosynthesis genes and nucleosome assembly genes. *J. Biol. Rhythms* 21:350–361.

Panda S, Hogenesch JB. (2004). It's all in the timing: many clocks, many outputs. *J. Biol. Rhythms* 19:374–387.

Panda S, Antoch MP, Miller BH, Su AI, Schook AB, Straume M, Schultz PG, Kay SA, Takahashi JS, Hogenesch JB. (2002). Coordinated transcription of key pathways in the mouse by the circadian clock. *Cell* 109:307–320.

Portaluppi F, Smolensky MH, Touitou Y. (2010). Ethics and methods for biological rhythm research on animals and human beings. *Chronobiol. Int.* 27:1911–1929.

Preitner N, Damiola F, Lopez-Molina L, Zakany J, Duboule D, Albrecht U, Schibler U. (2002). The orphan nuclear receptor REV-ERBalpha controls circadian transcription within the positive limb of the mammalian circadian oscillator. *Cell* 110:251–260.

Reppert SM, Weaver DR. (2002). Coordination of circadian timing in mammals. *Nature* 418:935–941.

Rey G, Cesbron F, Rougemont J, Reinke H, Brunner M, Naef F. (2011). Genome-wide and phase-specific DNA-binding rhythms of BMAL1 control circadian output functions in mouse liver. *PLoS Biol.* 9: pe1000595.

Sammar M, Gulbins E, Hilbert K, Lang F, Altevogt P. (1997). Mouse CD24 as a signaling molecule for integrin-mediated cell binding: functional and physical association with src-kinases. *Biochem. Biophys. Res. Commun.* 234:330–334.

Sato TK, Yamada RG, Ukai H, Baggs JE, Miraglia LJ, Kobayashi TJ, Welsh DK, Kay SA, Ueda HR, Hogenesch JB. (2006). Feedback repression is required for mammalian circadian clock function. *Nat. Genet.* 38:312–319.

Sherman BT, Huang da W, Tan Q, Guo Y, Bour S, Liu D, Stephens R, Baseler MW, Lane HC, Lempicki RA. (2007). DAVID Knowledgebase: a gene-centered database integrating heterogeneous gene annotation resources to facilitate high-throughput gene functional analysis. *BMC Bioinformatics* 8:426.

Shewan D, Calaora V, Nielsen P, Cohen J, Rougon G, Moreau H. (1996). mCD24, a glycoprotein transiently expressed by neurons, is an inhibitor of neurite outgrowth. *J. Neurosci.* 16:2624–2634.

Smith M, Burke Z, Humphries A, Wells T, Klein D, Carter D, Baler R. (2001). Tissue-specific transgenic knockdown of Fos-related antigen 2 (Fra-2) expression mediated by dominant negative Fra-2. *Mol. Cell Biol.* 21:3704–3713.

Storch K-F, Lipan O, Leykin I, Viswanathan N, Davis FC, Wong WH, Weitz CJ. (2002). Extensive and divergent circadian gene expression in liver and heart. *Nature* 417:78–83.

Storch KF, Paz C, Signorovitch J, Raviola E, Pawlyk B, Li T, Weitz CJ. (2007). Intrinsic circadian clock of the mammalian retina: importance for retinal processing of visual information. *Cell* 130:730–741.

Takahashi JS. (2004). Finding new clock components: past and future. *J. Biol. Rhythms* 19:339–347.

Tanaka K, Murakami M, Greer MA. (1987). Rhythmicity of triiodothyronine generation by type II thyroxine 5'-deiodinase in rat pineal is mediated by a beta-adrenergic mechanism. *Endocrinology* 121:74–77.

Triqueneaux G, Thenot S, Kakizawa T, Antoch MP, Safi R, Takahashi JS, Delaunay F, Laudet V. (2004). The orphan receptor Rev-erbalpha gene is a target of the circadian clock pacemaker. *J. Mol. Endocrinol.* 33:585–608.

Ueda HR, Chen W, Adachi A, Wakamatsu H, Hayashi S, Takasugi T, Nagano M, Nakahama K-I, Suzuki Y, Sugano S, Iino M, Shigeyoshi Y, Hashimoto S. (2002). A transcription factor response element for gene expression during circadian night. *Nature* 418:534–539.

Yamato M, Ito T, Iwatani H, Yamato M, Imai E, Rakugi H. (2010). E-cadherin and claudin-4 expression has circadian rhythm in adult rat kidney. *J. Nephrol.* 23:102–110.

Yang Q, Graham TE, Mody N, Preitner F, Peroni OD, Zabolotny JM, Kotani K, Quadro L, Kahn BB. (2005). Serum retinol binding protein 4 contributes to insulin resistance in obesity and type 2 diabetes. *Nature* 436:356–362.

Yoo SH, Yamazaki S, Lowrey PL, Shimomura K, Ko CH, Buhr ED, Siepka SM, Hong HK, Oh WJ, Yoo OJ, Menaker M, Takahashi JS (2004). PERIOD2::LUCIFERASE real-time reporting of circadian dynamics reveals persistent circadian oscillations in mouse peripheral tissues. *Proc. Natl. Acad. Sci. U. S. A.* 101:5339–5346.

SUPPLEMENTARY FIGURE 1. Pathways identified by KEGG Classification System analysis for the 252 significantly altered genes in *Bmal1* knockdown pituitary glands. The altered genes are indicated by *.

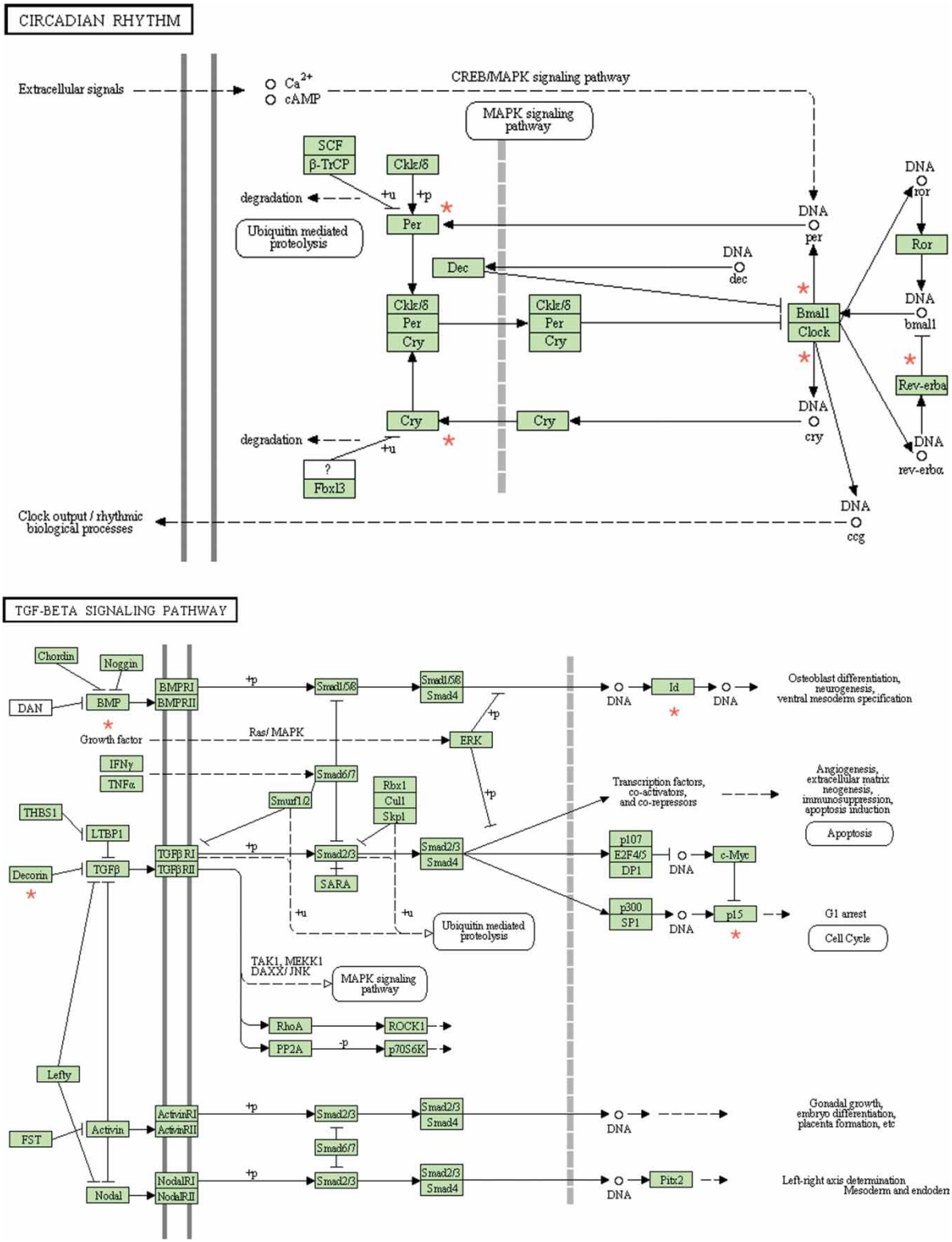

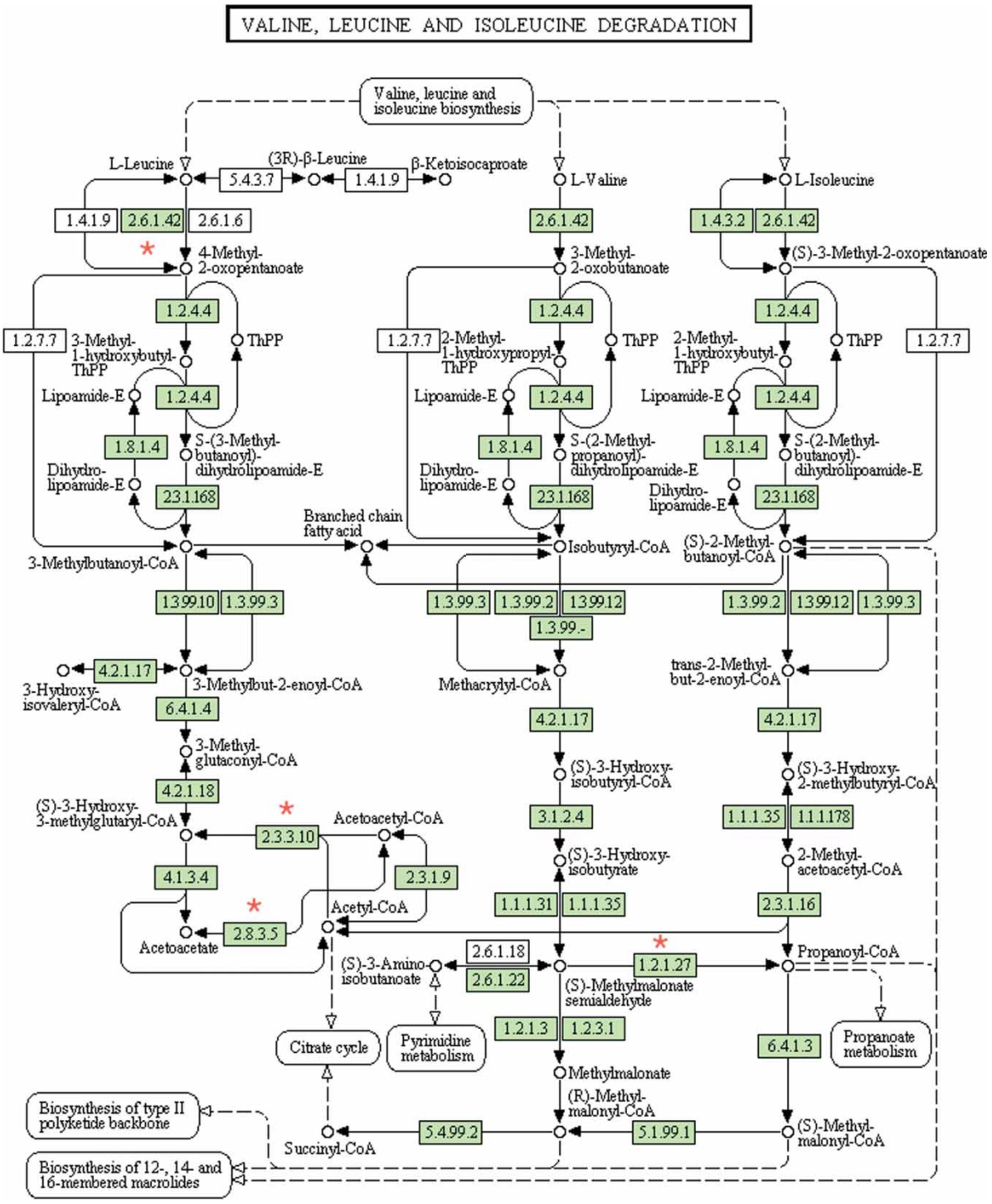

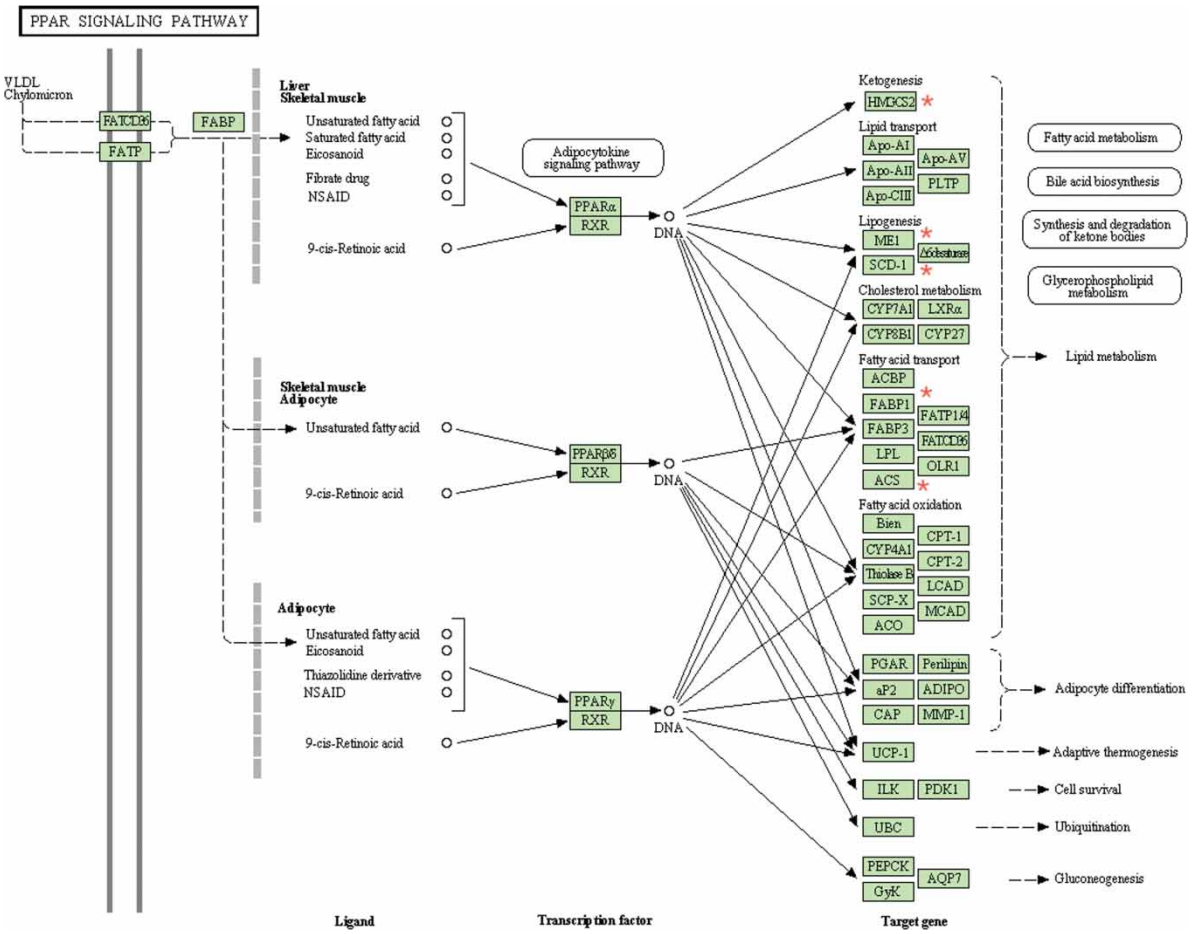

SUPPLEMENTARY TABLE 1. Primer list (5′ to 3′) for qPCR mRNA analyses

Bmal1	TGACCCTCATGGAAGGTTAGAA CAGCCATCCTTAGCACGGT
Clock	CTTCCTGGTAACGCGAGAAAG TCGAATCTCACTAGCATCTGACT
Npas2	AAGGATAGAGCAAAGAGAGCCT CATTTTCCGAGTGTTACCAGGG
Rorγ	GACCCACACCTCACAAATTGA AGTAGGCCACATTACACTGCT
Reverbα	TACATTGGCTCTAGTGGCTCC CAGTAGGTGATGGTGGGAAGTA
Dio2	AATTATGCCTCGGAGAAGACCG GGCAGTTGCCTAGTGAAAGGT
Rbp4	AGTCAAGGAGAACTTCGACAAGG CAGAAAACTCAGCGATGATGTTG
Tef	GAACAATGTGGCAGCTAAACGC TCTCGTACTTGGACACGATGGTCT
Cd24a	GTTGCACCGTTTCCCGGTAA CCCCTCTGGTGGTAGCGTTA
Cntn1	TTTCATCCCTGCTCAGAGGATGCT CTGAATGCCTCAGTCGTGATGTGT
36B4	GCTGATGGGCAAGAACACCA CCCAAAGCCTGGAAGAAGGA

SUPPLEMENTARY TABLE 2. Genes modified in pituitaries from *Bmal1*$^{-/-}$ knockout versus wild-type mice

Gene ID	Gene symbol	Accession Number	Coverage	Log-fold change	% change
68616	Gdpd3	NM_024228	9	1.830000043	356%
18143	Npas2	NM_008719	13	1.350000024	255%
12952	Cry1	NM_007771	9	1.309999943	248%
	—	NM_001113013	10	1.169999957	225%
27226	Pla2g7	NM_013737	10	1.169999957	225%
18133	Nov	NM_010930	15	1.110000014	216%
19885	Rorc	NM_011281	15	1.100000024	214%
105387	Akr1c14	NM_134072	3	1.080000043	211%
	—	ENSMMUT00000022992	10	1.070000052	210%
12140	Fabp7	NM_021272	3	1.070000052	210%
70186	Fam162a	NM_027342	10	1.070000052	210%
	—	ENSRNOT00000020443	7	1.019999981	203%
	—	XM_001101603	10	1	200%
231440	9130213B05Rik	NM_145562	10	1	200%
	—	XM_001088804	11	.970000029	196%
	—	XM_001924188	11	.970000029	196%
80837	Rhoj	NM_023275	10	.949999988	193%
	—	ENSECAT00000026609	8	.930000007	191%
	—	ENSCAFT00000020154	8	.930000007	191%
12805	Cntn1	NM_001159647	20	.920000017	189%
13371	Dio2	NM_010050	19	.920000017	189%
26897	Acot1	NM_012006	3	.850000024	180%
15904	Id4	NM_031166	13	.850000024	180%
100044830	LOC100044830	XR_031056	3	.850000024	180%
	—	AK296896	3	.839999974	179%
11304	Abca4	NM_007378	3	.839999974	179%
	—	NM_001106306	12	.829999983	178%
55987	Cpxm2	NM_018867	12	.829999983	178%
100048724	LOC100048724	XM_001481056	9	.829999983	178%
30049	Scd3	NM_024450	9	.829999983	178%
	—	NM_001135088	7	.810000002	175%
12709	Ckb	NM_021273	4	.810000002	175%
100046232	LOC100046232	XM_001475817	6	.810000002	175%
18109	Mycn	NM_008709	11	.810000002	175%
18030	Nfil3	NM_017373	6	.810000002	175%
29813	Zfp385a	NM_013866	7	.810000002	175%
	—	XM_001109930	6	.790000021	173%
	—	XM_001110067	6	.790000021	173%
100045546	LOC100045546	XM_001474498	15	.790000021	173%
18619	Penk	NM_001002927	6	.790000021	173%
	—	ENSMMUT00000031972	12	.779999971	172%
11737	Anp32a	NM_009672	12	.779999971	172%
18791	Plat	NM_008872	9	.779999971	172%
232023	Vopp1	NM_146168	18	.779999971	172%
11861	Arl4a	NM_007487	7	.769999981	171%
114249	Npnt	ENSMUST00000117811	13	.769999981	171%
70097	Sash1	NM_175155	7	.769999981	171%
	—	ENSMMUT00000004155	9	.75999999	169%
21833	Thra	ENSMUST00000064187	9	.75999999	169%
19378	Aldh1a2	NM_009022	9	.75	168%
12484	Cd24a	NM_009846	12	.75	168%
18012	Neurod1	NM_010894	5	.75	168%
65255	Asb4	NM_023048	17	.74000001	167%
23965	Odz3	NM_011857	3	.74000001	167%
	—	ENSPTRT00000029090	9	.730000019	166%
	—	ENSMMUT00000018254	12	.730000019	166%
102545	Cmtm7	NM_133978	6	.720000029	165%
	—	ENSPTRT00000047260	8	.709999979	164%
	—	AK128317	8	.709999979	164%
	—	ENSMMUT00000013530	8	.709999979	164%
11865	Arntl	NM_007489	8	.709999979	164%
12579	Cdkn2b	NM_007670	4	.699999988	162%
15901	Id1	NM_010495	3	.699999988	162%

Continued

SUPPLEMENTARY TABLE 2. Continued

Gene ID	Gene symbol	Accession Number	Coverage	Log-fold change	% change
12161	Bmp6	AK135770	9	.689999998	161%
637082	LOC637082	XM_916287	7	.689999998	161%
211550	Tifa	NM_145133	7	.689999998	161%
217410	Trib2	NM_144551	5	.689999998	161%
	—	ENSMMUT00000030973	7	.680000007	160%
	—	XM_001100872	3	.680000007	160%
67731	Fbxo32	NM_026346	3	.680000007	160%
12587	Mia1	NM_019394	8	.680000007	160%
78593	Nrip3	NM_020610	12	.680000007	160%
	—	ENSCAFT00000036906	6	.670000017	159%
	—	NM_001030025	3	.670000017	159%
	—	ENSECAT00000008545	3	.670000017	159%
	—	XM_001497898	3	.670000017	159%
27528	D0H4S114	NM_053078	8	.670000017	159%
100047936	LOC100047936	XR_033905	9	.670000017	159%
20713	Serpini1	NM_009250	18	.670000017	159%
20660	Sorl1	NM_011436	9	.670000017	159%
67971	Tppp3	NM_026481	6	.670000017	159%
22271	Upp1	NM_009477	3	.670000017	159%
12753	Clock	NM_007715	6	.660000026	158%
67213	Cmtm6	NM_026036	3	.660000026	158%
56183	Nmu	NM_019515	5	.660000026	158%
21928	Tnfaip2	NM_009396	3	.660000026	158%
100045882	LOC100045882	XM_001475083	4	.649999976	157%
19736	Rgs4	NM_009062	9	.649999976	157%
20516	Slc20a2	NM_011394	4	.649999976	157%
22627	Ywhae	NM_009536	5	.649999976	157%
231238	2310045A20Rik	NM_172710	3	.639999986	156%
12826	Col4a1	NM_009931	7	.639999986	156%
232680	Cpa2	NM_001024698	7	.639999986	156%
17118	Marcks	ENSMUST00000092584	13	.639999986	156%
218121	Mboat1	NM_153546	3	.639999986	156%
70155	Ogfrl1	NM_001081079	4	.639999986	156%
19274	Ptprm	NM_008984	4	.639999986	156%
70747	Tspan2	NM_027533	3	.639999986	156%
	—	ENSMMUT00000006964	10	.629999995	155%
	—	XM_541259	9	.629999995	155%
	—	XM_001074064	4	.629999995	155%
69635	Dapk1	NM_029653	10	.629999995	155%
14704	Gng3	NM_010316	4	.629999995	155%
17762	Mapt	NM_001038609	5	.629999995	155%
56421	Pfkp	NM_019703	10	.629999995	155%
19277	Ptpro	NM_011216	8	.629999995	155%
68939	Rasl11b	NM_026878	6	.629999995	155%
214359	Tmem51	NM_145402	5	.629999995	155%
	—	ENST00000368075	9	.620000005	154%
71994	Cnn3	AK051628	12	.620000005	154%
15902	Id2	NM_010496	12	.620000005	154%
677317	LOC677317	XM_001004685	4	.620000005	154%
17436	Me1	NM_008615	4	.620000005	154%
18007	Neo1	NM_008684	5	.620000005	154%
57319	Smpdl3a	NM_020561	7	.620000005	154%
74413	Tc2n	NM_028924	5	.620000005	154%
22194	Ube2e1	NM_009455	4	.620000005	154%
	—	XM_001077447	4	.610000014	153%
	—	ENSPTRT00000066250	7	.610000014	153%
	—	NM_001107463	15	.610000014	153%
	—	ENSMMUT00000025070	19	.610000014	153%
11747	Anxa5	NM_009673	9	.610000014	153%
13713	Elk3	NM_013508	3	.610000014	153%
15360	Hmgcs2	NM_008256	8	.610000014	153%
20185	Ncor1	ENSMUST00000037575	4	.610000014	153%
18582	Pde6d	NM_008801	7	.610000014	153%
18611	Pea15a	NM_011063	20	.610000014	153%

Continued

SUPPLEMENTARY TABLE 2. Continued

Gene ID	Gene symbol	Accession Number	Coverage	Log-fold change	% change
218756	Slc4a7	NM_001033270	3	.610000014	153%
20677	Sox4	AK031394	8	.610000014	153%
68539	Tmem109	NM_134142	7	.610000014	153%
107305	Vps37c	AK159309	15	.610000014	153%
	—	ENSBTAT00000054711	3	−.50999999	70%
	—	ENST00000342945	4	−.50999999	70%
67373	2210010C04Rik	NM_023333	3	−.50999999	70%
11722	Amy1	ENSMUST00000106536	3	−.50999999	70%
12035	Bcat1	NM_007532	4	−.50999999	70%
66205	Cd302	NM_025422	5	−.50999999	70%
26427	Creb3l1	NM_011957	4	−.50999999	70%
13034	Ctse	NM_007799	3	−.50999999	70%
73284	Ddit4l	AK029362	9	−.50999999	70%
14799	Gria1	NM_001113325	8	−.50999999	70%
15972	Ifna9	NM_010507	3	−.50999999	70%
16493	Kcna5	NM_145983	4	−.50999999	70%
100044431	LOC100044431	XM_001472241	8	−.50999999	70%
100046168	LOC100046168	XM_001475723	3	−.50999999	70%
70152	Mettl7a1	NM_027334	9	−.50999999	70%
65113	Ndfip1	ENSMUST00000025293	3	−.50999999	70%
18484	Pam	NM_013626	4	−.50999999	70%
216134	Pdxk	AK009645	6	−.50999999	70%
18610	Pdyn	AK133597	3	−.50999999	70%
19737	Rgs5	NM_009063	13	−.50999999	70%
67225	Rnpc3	NM_001038696	3	−.50999999	70%
20491	Sla	NM_001029841	3	−.50999999	70%
71929	Tmem123	NM_133739	7	−.50999999	70%
	—	XM_001501998	7	−.519999981	70%
	—	ENSCAFT00000029512	5	−.519999981	70%
	—	NM_001076070	5	−.519999981	70%
	—	ENSMMUT00000033381	4	−.519999981	70%
	—	AK298352	5	−.519999981	70%
	—	ENSECAT00000021139	5	−.519999981	70%
12516	Cd7	NM_009854	3	−.519999981	70%
13690	Eif4g2	NM_001040131	3	−.519999981	70%
224093	Fam43a	NM_177632	3	−.519999981	70%
14168	Fgf13	NM_010200	8	−.519999981	70%
108682	Gpt2	NM_173866	13	−.519999981	70%
16336	Insl3	NM_013564	4	−.519999981	70%
16453	Jak3	NM_010589	4	−.519999981	70%
100045442	LOC100045442	XM_001474252	3	−.519999981	70%
75746	Morc4	ENSMUST00000113017	7	−.519999981	70%
219135	Mtmr6	NM_144843	5	−.519999981	70%
67041	Oxct1	NM_024188	5	−.519999981	70%
67375	Qprt	NM_133686	3	−.519999981	70%
20842	Stag1	NM_009282	3	−.519999981	70%
72003	Synpr	NM_001163032	4	−.519999981	70%
22402	Wisp1	NM_018865	8	−.519999981	70%
	—	XM_861214	8	−.529999971	69%
	—	NM_001106858	3	−.529999971	69%
	—	ENSMMUT00000007303	14	−.529999971	69%
66214	1190002H23Rik	NM_025427	13	−.529999971	69%
104776	Aldh6a1	NM_134042	4	−.529999971	69%
73834	Atp6v1d	NM_023721	3	−.529999971	69%
72605	Car10	NM_028296	8	−.529999971	69%
12836	Col7a1	NM_007738	3	−.529999971	69%
14219	Ctgf	NM_010217	6	−.529999971	69%
13179	Dcn	NM_007833	10	−.529999971	69%
17263	Meg3	AK148955	4	−.529999971	69%
14815	Nr3c1	NM_008173	5	−.529999971	69%
70536	Qpct	NM_027455	5	−.529999971	69%
103655	Sec14l4	NM_146013	9	−.529999971	69%
213053	Slc39a14	NM_001135151	9	−.529999971	69%
21841	Tia1	NM_011585	3	−.529999971	69%

Continued

SUPPLEMENTARY TABLE 2. Continued

Gene ID	Gene symbol	Accession Number	Coverage	Log-fold change	% change
	—	ENSMMUT00000025501	3	−.540000021	69%
	—	AK122702	3	−.540000021	69%
	—	AK074203	11	−.540000021	69%
	—	AK022558	3	−.540000021	69%
	—	NM_017168	9	−.540000021	69%
	—	XM_855316	3	−.540000021	69%
	—	ENSBTAT00000002717	9	−.540000021	69%
74653	4930444A02Rik	NM_029037	4	−.540000021	69%
216739	Acsl6	NM_001033599	3	−.540000021	69%
11733	Ank1	NM_001110783	3	−.540000021	69%
18720	Pip5k1a	ENSMUST00000107235	3	−.540000021	69%
234779	Plcg2	NM_172285	9	−.540000021	69%
69048	Slc30a5	NM_022885	3	−.540000021	69%
20983	Syt4	NM_009308	6	−.540000021	69%
	—	NM_012648	9	−.550000012	68%
	—	ENSCAFT00000008641	6	−.550000012	68%
	—	ENST00000440169	5	−.550000012	68%
	—	ENST00000443804	5	−.550000012	68%
	—	XM_850653	3	−.550000012	68%
	—	ENSMODT00000010563	4	−.550000012	68%
67313	5730559C18Rik	AK017848	3	−.550000012	68%
11529	Adh7	NM_009626	3	−.550000012	68%
12457	Ccrn4l	NM_009834	4	−.550000012	68%
13647	Egfbp2	NM_010115	9	−.550000012	68%
26912	Gcat	NM_013847	3	−.550000012	68%
16009	Igfbp3	NM_008343	3	−.550000012	68%
16511	Kcnh2	NM_013569	3	−.550000012	68%
16618	Klk1b26	NM_010644	9	−.550000012	68%
100046101	LOC100046101	XR_032310	9	−.550000012	68%
100047076	LOC100047076	XM_001477348	3	−.550000012	68%
100047134	LOC100047134	XM_001477322	4	−.550000012	68%
230082	Nol6	NM_139236	3	−.550000012	68%
18227	Nr4a2	NM_013613	3	−.550000012	68%
18645	Pfn2	NM_019410	4	−.550000012	68%
20277	Scnn1b	NM_011325	9	−.550000012	68%
19720	Trim27	NM_009054	5	−.550000012	68%
22110	Tspyl1	NM_009433	3	−.550000012	68%
72088	Ush1c	NM_001163733	5	−.550000012	68%
	—	XM_001097119	12	−.560000002	68%
	—	ENSRNOT00000056670	6	−.560000002	68%
	—	ENSRNOT00000056671	6	−.560000002	68%
233913	BC017158	NM_145590	4	−.560000002	68%
214498	Cdc73	AK029710	5	−.560000002	68%
107526	Gimap4	NM_174990	3	−.560000002	68%
64242	Ngb	NM_022414	7	−.560000002	68%
69806	Slc39a11	NM_027216	7	−.560000002	68%
212980	Slc45a3	NM_145977	15	−.560000002	68%
22239	Ugt8a	NM_011674	12	−.560000002	68%
	—	XM_001087516	4	−.569999993	67%
	—	ENSRNOT00000016242	4	−.569999993	67%
	—	XM_001164096	4	−.569999993	67%
	—	AK025962	4	−.569999993	67%
20312	Cx3cl1	NM_009142	16	−.569999993	67%
223527	Eny2	NM_175009	4	−.569999993	67%
14229	Fkbp5	NM_010220	12	−.569999993	67%
16615	Klk1b16	NM_008454	8	−.569999993	67%
677606	LOC677606	XR_035067	8	−.569999993	67%
217734	Pomt2	NM_153415	4	−.569999993	67%
108705	Pttg1ip	NM_145925	3	−.569999993	67%
52118	Pvr	AK080753	4	−.569999993	67%
51801	Ramp1	NM_016894	8	−.569999993	67%
21859	Timp3	NM_011595	24	−.569999993	67%
66676	Tmed7	NM_025698	3	−.569999993	67%

Continued

SUPPLEMENTARY TABLE 2. Continued

Gene ID	Gene symbol	Accession Number	Coverage	Log-fold change	% change
64540	Tspan4	NM_053082	7	−.569999993	67%
53376	Usp2	NM_016808	18	−.569999993	67%
75581	Yipf7	NM_023784	3	−.569999993	67%
	—	ENSMMUT00000038891	8	−.579999983	67%
	—	ENSRNOT00000025916	6	−.579999983	67%
494504	Apcdd1	AK172004	3	−.579999983	67%
497653	BE136769	AK080269	5	−.579999983	67%
67800	Dgat2	NM_026384	15	−.579999983	67%
13612	Edil3	NM_001037987	3	−.579999983	67%
66629	Golph3	NM_025673	4	−.579999983	67%
15387	Hnrnpk	AK135519	6	−.579999983	67%
66277	Klf15	NM_023184	4	−.579999983	67%
676708	LOC676708	XM_992322	5	−.579999983	67%
233575	Pgap2	ENSMUST00000120119	6	−.579999983	67%
21817	Tgm2	NM_009373	41	−.579999983	67%
	—	NM_001135785	3	−.589999974	66%
80794	Cblc	NM_023224	3	−.589999974	66%
13107	Cyp2f2	NM_007817	9	−.589999974	66%
13808	Eno3	NM_007933	5	−.589999974	66%
14038	Expi	NM_007969	3	−.589999974	66%
320806	Gfm2	AK052633	3	−.589999974	66%
226896	Tcfap2d	NM_153154	3	−.589999974	66%
21685	Tef	NM_017376	15	−.589999974	66%
22390	Wee1	NM_009516	5	−.589999974	66%
50926	Hnrpdl	NM_016690	16	−.600000024	66%
53381	Prdx4	NM_016764	3	−.600000024	66%
71690	Esm1	NM_023612	3	−.610000014	66%
14711	Gnmt	NM_010321	9	−.610000014	66%
20887	Sult1a1	NM_133670	9	−.610000014	66%
	—	AK296027	13	−.620000005	65%
18606	Enpp2	NM_015744	13	−.620000005	65%
20320	Nptn	NM_009145	3	−.620000005	65%
20606	Sstr2	ENSMUST00000106630	3	−.620000005	65%
12608	Cebpb	NM_009883	7	−.629999995	65%
14582	Gfi1b	NM_001160406	4	−.629999995	65%
22634	Plagl1	NM_009538	3	−.629999995	65%
	—	XM_001375167	5	−.649999976	64%
16530	Kcnk7	NM_010609	3	−.649999976	64%
16619	Klk1b27	NM_020268	6	−.649999976	64%
94094	Trim34	NM_030684	7	−.649999976	64%
	—	XM_001087953	11	−.660000026	63%
	—	AK057480	11	−.660000026	63%
	—	ENSRNOT00000028447	3	−.660000026	63%
21802	Tgfa	NM_031199	4	−.660000026	63%
12570	Cdk5r2	ENSMUST00000006718	10	−.680000007	62%
53379	Hnrnpa2b1	NM_016806	4	−.680000007	62%
18628	Per3	NM_011067	10	−.680000007	62%
26943	Serinc3	NM_012032	6	−.680000007	62%
22409	Wnt10a	NM_009518	9	−.689999998	62%
11685	Alox12e	NM_145684	7	−.699999988	62%
66102	Cxcl16	NM_023158	3	−.699999988	62%
70935	Speer4f	NM_027609	3	−.709999979	61%
14419	Gal	NM_010253	6	−.720000029	61%
	—	ENSPTRT00000012674	8	−.730000019	60%
23892	Grem1	NM_011824	8	−.730000019	60%
	—	ENSRNOT00000020425	4	−.74000001	60%
	—	AK293273	4	−.74000001	60%
15483	Hsd11b1	NM_008288	9	−.74000001	60%
74747	Ddit4	NM_029083	8	−.769999981	59%
110058	Syt17	AK144560	5	−.769999981	59%
20295	Ccl17	NM_011332	3	−.790000021	58%
	—	ENSTGUT00000003479	3	−.800000012	57%
17313	Mgp	NM_008597	8	−.800000012	57%
	—	NM_001081951	9	−.850000024	55%

Continued

SUPPLEMENTARY TABLE 2. Continued

Gene ID	Gene symbol	Accession Number	Coverage	Log-fold change	% change
	—	ENSRNOT00000021055	9	−.850000024	55%
100047573	LOC100047573	XM_001478425	9	−.850000024	55%
19662	Rbp4	NM_001159487	9	−.850000024	55%
26366	Ceacam10	NM_007675	17	−.910000026	53%
104158	Ces3	NM_053200	23	−.980000019	51%
16819	Lcn2	NM_008491	10	−.980000019	51%
20720	Serpine2	NM_009255	11	−.980000019	51%
18704	Pik3c2a	NM_011083	3	−.99000001	50%
217166	Nr1d1	NM_145434	8	−1.019999981	49%
20750	Spp1	NM_009263	9	−1.070000052	48%
	—	XR_028882	6	−1.110000014	46%
54208	Arl6ip1	NM_019419	4	−1.110000014	46%
13170	Dbp	NM_016974	20	−1.379999995	38%
353187	Nr1d2	NM_011584	12	−1.99000001	25%

SUPPLEMENTARY TABLE 3. Overlap between genes with altered expression in *Bmal1*$^{-/-}$ mouse pituitary and circadian pituitary transcriptome (Hughes et al., 2010)

Genes unique to the list of pituitary CCGs (Hughes et al., 2010; 290 items)	Genes unique to the list of altered genes in *Bmal1*$^{-/-}$ mouse pituitary (199 items)	Genes common to the two lists (53 items)
0610031G08Rik	2210010C04Rik	1190002H23Rik
1110002L01Rik	2310045A20Rik	Alox12e
1110019N10Rik	4930444A02Rik	Arl4a
1110039B18Rik	5730559C18Rik	Arntl
1110051B16Rik	9130213B05Rik	Bmp6
1200013P24Rik	Abca4	Cd24a
1500004A08Rik	Acot1	Ces3
1500009M05Rik	Acsl6	Clock
1500041J02Rik	Adh7	Cmtm7
1700023A16Rik	Akr1c14	Col4a1
1810013L24Rik	Aldh1a2	Cry1
1810053B01Rik	Aldh6a1	Ctgf
1810055G02Rik	Amy1	Cx3cl1
1810057P16Rik	Ank1	Cyp2f2
1810062G17Rik	Anp32a	D0H4S114
2010300C02Rik /// LOC639555	Anxa5	Dapk1
2210038L17Rik	Apcdd1	Dbp
2310003C23Rik	Arl6ip1	Ddit4l
2310015B20Rik	Asb4	Dgat2
2310056P07Rik	Atp6v1d	Eno3
2410014A08Rik	BC017158	Fkbp5
2410016F19Rik	Bcat1	Hmgcs2
2610044O15Rik	BE136769	Hnrpdl
2610201A13Rik	Car10	Igfbp3
2700055K07Rik	Cblc	Klf15
2810002D19Rik	Ccl17	Klk1b26
2900052N01Rik	Ccrn4l	Klk1b27
4631416L12Rik	Cd302	Mycn
4833417J20Rik	Cd7	Nfil3
4930447M23Rik	Cdc73	Ngb
4930469P12Rik	Cdk5r2	Nov
4930526H21Rik	Cdkn2b	Npas2
4933407H18Rik	Ceacam10	Npnt
5430407P10Rik	Cebpb	Nr1d1
5730405I09Rik	Ckb	Nr1d2
5730596K20Rik	Cmtm6	Pdxk
6330404F12Rik	Cnn3	Per3
6330406I15Rik	Cntn1	Pla2g7

Continued

SUPPLEMENTARY TABLE 3. Continued

Genes unique to the list of pituitary CCGs (Hughes et al., 2010; 290 items)	Genes unique to the list of altered genes in *Bmal1*$^{-/-}$ mouse pituitary (199 items)	Genes common to the two lists (53 items)
6330514A18Rik	Col7a1	Plat
8430426J06Rik	Cpa2	Rasl11b
9230117N10Rik	Cpxm2	Rorc
A330049M08Rik	Creb3l1	Scd3
A330094K24Rik	Ctse	Sec14l4
A430065P19Rik	Cxcl16	Slc39a14
A630005I04Rik	Dcn	Sult1a1
AA536717	Ddit4	Tef
Aass	Dio2	Thra
Abcc5	Edil3	Timp3
Abcd2	Egfbp2	Tnfaip2
Abhd8	Eif4g2	Tspan4
Acat1	Elk3	Usp2
Acss2	Enpp2	Vps37c
Actn1	Eny2	Wee1
Actn2	Esm1	
Adcy7	Expi	
AF529169	Fabp7	
Agtrl1	Fam162a	
Ahsa1	Fam43a	
AI848100	Fbxo32	
Ak3	Fgf13	
Aldh1a1	Gal	
Aldh1l1	Gcat	
Aldh7a1	Gdpd3	
Aldh9a1	Gfi1b	
Aldoc	Gfm2	
Alg8	Gimap4	
Alox15	Gng3	
Angpt1	Gnmt	
Ankrd12	Golph3	
Antxr2	Gpt2	
Ap1s2	Grem1	
Aqp11	Gria1	
Arf4	Hnrnpa2b1	
Asb14	Hnrnpk	
Asphd2	Hsd11b1	
AU040829	Id1	
AU044698	Id2	
AU067824	Id4	
AW547186	Ifna9	
B230114P17Rik	Insl3	
Banf1	Jak3	
BC008163	Kcna5	
BC027342	Kcnh2	
BC034090	Kcnk7	
BC055107	Klk1b16	
BC062258	Lcn2	
BF642829	LOC100044431	
C030045D06Rik	LOC100044830	
Camkk2	LOC100045442	
Canx	LOC100045546	
Cbr2	LOC100045882	
Ccbe1	LOC100046101	
Ccbl1	LOC100046168	
Ccdc85b	LOC100046232	
Ccnjl	LOC100047076	
Cdc42ep2	LOC100047134	
Cebpd	LOC100047573	
Chchd7	LOC100047936	
Chordc1	LOC100048724	
Cilp	LOC637082	

Continued

SUPPLEMENTARY TABLE 3. Continued

Genes unique to the list of pituitary CCGs (Hughes et al., 2010; 290 items)	Genes unique to the list of altered genes in *Bmal1*$^{-/-}$ mouse pituitary (199 items)	Genes common to the two lists (53 items)
Cited1	LOC676708	
Cldn12	LOC677317	
Cmtm3	LOC677606	
Colec11	Mapt	
Cpt1a	Marcks	
Creld2	Mboat1	
Cry2	Me1	
Cryzl1	Meg3	
Cybrd1	Mettl7a1	
Cyp2a4 /// Cyp2a5	Mgp	
Cys1	Mia1	
D15Bwg0759e	Morc4	
D17Wsu104e	Mtmr6	
D3Ertd300e	Ncor1	
D7Wsu130e	Ndfip1	
Ddah1	Neo1	
Dhtkd1	Neurod1	
Dip2a	Nmu	
Dnahc9	Nol6	
Dnajc10	Nptn	
Doc2b	Nr3c1	
Dpys	Nr4a2	
Dtx4	Nrip3	
Dynll1	Odz3	
Dynlrb2	Ogfrl1	
Ednrb	Oxct1	
Egfl7	Pam	
Eif5	Pde6d	
Enc1	Pdyn	
Ephx1	Pea15a	
Etv1	Penk	
Etv5	Pfkp	
Fhit	Pfn2	
Fmo1	Pgap2	
Fmo2	Pik3c2a	
Fut2	Pip5k1a	
Fyn	Plagl1	
Fzd3	Plcg2	
G0s2	Pomt2	
Galntl4	Prdx4	
Gas1	Ptprm	
Gldc	Ptpro	
Glul	Pttg1ip	
Gm129	Pvr	
Gnai1	Qpct	
Gnas	Qprt	
Gnb3	Ramp1	
Gpihbp1	Rbp4	
Gpr149	Rgs4	
Gpr155	Rgs5	
Gpr68	Rhoj	
Gpr83	Rnpc3	
Gstk1	Sash1	
H13	Scnn1b	
Hif3a	Serinc3	
Hist1h1e	Serpine2	
Hist1h3d	Serpini1	
Hist1h4h	Sla	
Hist1h4h /// Hist1h4c /// Hist1h4i /// Hist1h4j /// Hist1h4k /// Hist1h4m /// Hist1h4a /// Hist1h4b	Slc20a2	
Hist1h4i	Slc30a5	
Hist1h4j	Slc39a11	

Continued

SUPPLEMENTARY TABLE 3. Continued

Genes unique to the list of pituitary CCGs (Hughes et al., 2010; 290 items)	Genes unique to the list of altered genes in *Bmal1*$^{-/-}$ mouse pituitary (199 items)	Genes common to the two lists (53 items)
Hist2h2aa2	Slc45a3	
Hist2h2be	Slc4a7	
Hist2h3c1 /// Hist1h3f /// Hist1h3d /// Hist1h3b /// Hist1h3e /// Hist2h3b	Smpdl3a	
Hist2h3c2	Sorl1	
Hlf	Sox4	
Hnrpc	Speer4f	
Hnt	Spp1	
Hrk	Sstr2	
Hsp90aa1	Stag1	
Hspa1a	Synpr	
Hspa8 /// LOC621284 /// LOC666904	Syt17	
Hspb1	Syt4	
Ifit3	Tc2n	
Ifitm1	Tcfap2d	
Il22 /// Iltifb	Tgfa	
Iqsec3	Tgm2	
Itga6	Tia1	
Jam2	Tifa	
Jundm2	Tmed7	
Kcnj10	Tmem109	
Kitl	Tmem123	
Klf9	Tmem51	
Klk1b22 /// Klk1b9	Tppp3	
L3mbtl3	Trib2	
Leo1	Trim27	
Leprot	Trim34	
Lima1	Tspan2	
Lman2l	Tspyl1	
Lnx1	Ube2e1	
LOC217066	Ugt8a	
LOC622147 /// Env /// LOC668227 /// LOC668269 /// LOC669176 /// LOC669658 /// LOC669821 /// LOC676636	Upp1	
Lonrf1 /// LOC631639	Ush1c	
Lonrf3	Vopp1	
Lox	Wisp1	
Lrp8	Wnt10a	
Lrrc4	Yipf7	
Ly6c	Ywhae	
Mapk12	Zfp385a	
Mcm7		
Mettl7a		
Mettl7a /// Ubie		
Mlc1		
Mthfd1l		
Mtmr11		
Narg3		
Nmb		
Nptx1		
Nudt6		
Nup155		
Oact1		
Odf2		
Olig1		
Oplah		
P4ha2		
Parp3		
Pcbp2		
Pcdh12		
Peci		

Continued

SUPPLEMENTARY TABLE 3. Continued

Genes unique to the list of pituitary CCGs (Hughes et al., 2010; 290 items)	Genes unique to the list of altered genes in *Bmal1*$^{-/-}$ mouse pituitary (199 items)	Genes common to the two lists (53 items)
Per1		
Per2		
Plce1		
Plcl2		
Plekha4		
Plekhg4		
Por		
Prom1		
Psen2		
Ptgis		
Punc		
Pvalb		
Rasl10b		
Rasl11a		
Rassf8		
Rbbp8		
Rcor2		
Reck		
Rfc2		
Rhbdl2		
Rnasel		
Rps20 /// LOC245676 /// LOC623568		
Rsad1		
Rufy3		
Scn5a		
Serpine1		
Sez6		
Sfrp5		
Sfrs6		
Sin3b		
Slc16a12		
Slc38a2		
Slc41a3		
Slitrk6		
Smc6l1		
Snrk		
Sod2		
Sorcs1		
Spnb2		
Spred1		
Spsb3		
Stard5		
Stk35		
Sulf1		
Tardbp		
Tbx19		
Tieg3		
Tmem4		
Tmem57		
Tmhs		
Tmprss2		
Tor1aip2		
Tsc22d3		
Tshz2		
Tspan17		
Txnl4		
Ubie		
Uchl1		
Uhrf2		
Unc5d		
Usf2		
Vcam1		

Continued

SUPPLEMENTARY TABLE 3. Continued

Genes unique to the list of pituitary CCGs (Hughes et al., 2010; 290 items)	Genes unique to the list of altered genes in *Bmal1*$^{-/-}$ mouse pituitary (199 items)	Genes common to the two lists (53 items)
Vdac1		
Vps13a		
Wdr78		
Wnt9a		
Wwox		
Wwp2		
Ypel1		
Zbtb16		
Zfp191		

SUPPLEMENTARY TABLE 4. Gene – term enrichment analysis by DAVID functional annotation clustering

Annotation Cluster 1	Enrichment Score: 4.251710128342929			
Category	Term	Count	*p* value	fold enrichment
GOTERM_CC_FAT	GO:0044421~extracellular region part	29	2.21E-07	3.02
SP_PIR_KEYWORDS	signal	67	6.51E-07	1.81
GOTERM_CC_FAT	GO:0005576~extracellular region	44	1.44E-06	2.11
GOTERM_CC_FAT	GO:0005615~extracellular space	21	4.54E-06	3.32
SP_PIR_KEYWORDS	Secreted	39	4.86E-06	2.21
UP_SEQ_FEATURE	signal peptide	67	2.52E-05	1.63
SP_PIR_KEYWORDS	disulfide bond	48	0.001529445	1.56
SP_PIR_KEYWORDS	glycoprotein	62	0.004626086	1.39
UP_SEQ_FEATURE	disulfide bond	47	0.009967514	1.43
UP_SEQ_FEATURE	glycosylation site:N-linked (GlcNAc...)	60	0.037394837	1.26
Annotation Cluster 2	Enrichment Score: 3.383775081191144			
Category	Term	Count	*p* value	Fold enrichment
SP_PIR_KEYWORDS	biological rhythms	8	4.06E-09	30.64
GOTERM_BP_FAT	GO:0007623~circadian rhythm	8	6.52E-07	15.46
GOTERM_BP_FAT	GO:0048511~rhythmic process	11	1.04E-06	8.03
KEGG_PATHWAY	mmu04710:Circadian rhythm	6	1.23E-06	27.88
INTERPRO	IPR001610:PAC motif	5	2.72E-04	15.53
UP_SEQ_FEATURE	domain:PAC	5	3.01E-04	15.03
SMART	SM00086:PAC	5	3.50E-04	14.39
INTERPRO	IPR000014:PAS	5	6.17E-04	12.62
SMART	SM00091:PAS	5	7.92E-04	11.69
INTERPRO	IPR013655:PAS fold-3	4	0.001315593	17.94
UP_SEQ_FEATURE	domain:PAS 1	4	0.002131329	15.19
UP_SEQ_FEATURE	domain:PAS 2	4	0.002131329	15.19
INTERPRO	IPR001067:Nuclear translocator	3	0.003050615	34.60
BIOCARTA	m_circadianPathway:Circadian Rhythms	3	0.003229672	30.82
INTERPRO	IPR013767:PAS fold	4	0.004346482	11.96
INTERPRO	IPR011598:Helix-loop-helix DNA-binding	5	0.020951901	4.75
GOTERM_CC_FAT	GO:0005667~transcription factor complex	4	0.553047029	1.38
GOTERM_CC_FAT	GO:0044451~nucleoplasm part	5	0.881746668	.79
Annotation Cluster 3	Enrichment Score: 2.894707177680009			
Category	Term	Count	p value	Fold enrichment
UP_SEQ_FEATURE	DNA-binding region:Basic motif	10	2.89E-04	4.69
INTERPRO	IPR001092:Basic helix-loop-helix dimerisation region bHLH	8	4.52E-04	5.82
SMART	SM00353:HLH	8	6.56E-04	5.39
UP_SEQ_FEATURE	domain:Helix-loop-helix motif	8	7.83E-04	5.30
INTERPRO	IPR001067:Nuclear translocator	3	0.003050615	34.60
INTERPRO	IPR011598:Helix-loop-helix DNA-binding	5	0.020951901	4.75

Continued

SUPPLEMENTARY TABLE 4. Continued

Annotation Cluster 4	Enrichment Score: 2.6719416180280873			
Category	Term	Count	*p* value	Fold enrichment
INTERPRO	IPR001628:Zinc finger, nuclear hormone receptor-type	6	2.74E-04	10.31
INTERPRO	IPR001723:Steroid hormone receptor	6	3.03E-04	10.09
INTERPRO	IPR008946:Nuclear hormone receptor, ligand-binding	6	3.34E-04	9.89
INTERPRO	IPR000536:Nuclear hormone receptor, ligand-binding, core	6	3.34E-04	9.89
SMART	SM00399:ZnF_C4	6	3.70E-04	9.55
UP_SEQ_FEATURE	DNA-binding region:Nuclear receptor	6	4.13E-04	9.41
UP_SEQ_FEATURE	zinc finger region:NR C4-type	6	4.13E-04	9.41
SMART	SM00430:HOLI	6	4.50E-04	9.16
GOTERM_MF_FAT	GO:0003707~steroid hormone receptor activity	6	4.82E-04	9.09
INTERPRO	IPR013088:Zinc finger, NHR/GATA-type	6	4.83E-04	9.14
GOTERM_MF_FAT	GO:0004879~ligand-dependent nuclear receptor activity	6	8.96E-04	7.95
GOTERM_MF_FAT	GO:0043565~sequence-specific DNA binding	15	0.017451911	2.00
UP_SEQ_FEATURE	region of interest:Modulating	3	0.017672805	14.43
UP_SEQ_FEATURE	region of interest:Ligand-binding	3	0.060283706	7.47
SP_PIR_KEYWORDS	zinc finger	3	0.196766503	3.66
SP_PIR_KEYWORDS	zinc-finger	12	0.886716846	.80
Annotation Cluster 5	Enrichment Score: 2.410610096091163			
Category	Term	Count	*p* value	Fold enrichment
UP_SEQ_FEATURE	DNA-binding region:Basic motif	10	2.89E-04	4.69
INTERPRO	IPR011700:Basic leucine zipper	4	7.54E-04	21.53
INTERPRO	IPR004827:Basic-leucine zipper (bZIP) transcription factor	5	0.004390832	7.48
SMART	SM00338:BRLZ	5	0.005569031	6.93
UP_SEQ_FEATURE	domain:Leucine-zipper	6	0.016312686	4.05
GOTERM_MF_FAT	GO:0046983~protein dimerization activity	10	0.039601584	2.18
Annotation Cluster 6	Enrichment Score: 2.380807080852852			
Category	Term	Count	*p* value	Fold enrichment
INTERPRO	IPR000867:Insulin-like growth factor-binding protein, IGFBP	5	7.53E-05	21.25
UP_SEQ_FEATURE	domain:IGFBP N-terminal	5	9.26E-05	20.05
SMART	SM00121:IB	5	9.75E-05	19.70
GOTERM_MF_FAT	GO:0005520~insulin-like growth factor binding	5	1.89E-04	16.87
INTERPRO	IPR017891:Insulin-like growth factor binding protein, N-terminal	4	2.84E-04	29.36
INTERPRO	IPR012395:IGFBP-related, CNN	3	8.93E-04	60.56
PIR_SUPERFAMILY	PIRSF036495:IGFBP_rP_CNN	3	0.00151137	46.23
GOTERM_MF_FAT	GO:0019838~growth factor binding	6	0.002764774	6.19
UP_SEQ_FEATURE	domain:CTCK	4	0.002866574	13.75
INTERPRO	IPR006207:Cystine knot, C-terminal	4	0.003090349	13.46
SMART	SM00041:CT	4	0.003749474	12.47
INTERPRO	IPR006208:Cystine knot	3	0.006379527	24.22
GOTERM_BP_FAT	GO:0001558~regulation of cell growth	6	0.009158978	4.66
UP_SEQ_FEATURE	domain:TSP type-1	3	0.020016081	13.53
UP_SEQ_FEATURE	domain:VWFC	3	0.022481374	12.74
GOTERM_BP_FAT	GO:0040008~regulation of growth	8	0.066949794	2.23
INTERPRO	IPR001007:von Willebrand factor, type C	3	0.094541468	5.77
SMART	SM00214:VWC	3	0.106525026	5.35
INTERPRO	IPR000884:Thrombospondin, type 1 repeat	3	0.164617032	4.11
SMART	SM00209:TSP1	3	0.183895462	3.81
Annotation Cluster 7	Enrichment Score: 2.29222412355737			
Category	Term	Count	*p* value	Fold enrichment
GOTERM_BP_FAT	GO:0035295~tube development	11	0.003922182	2.98
GOTERM_BP_FAT	GO:0030324~lung development	7	0.00453208	4.51
GOTERM_BP_FAT	GO:0030323~respiratory tube development	7	0.004943597	4.43
GOTERM_BP_FAT	GO:0060541~respiratory system development	7	0.00771321	4.04

Continued

SUPPLEMENTARY TABLE 4. Continued

Annotation Cluster 8	Enrichment Score: 2.181590992415527			
Category	Term	Count	*p* value	Fold enrichment
GOTERM_MF_FAT	GO:0030295~protein kinase activator activity	4	4.76E-04	24.74
GOTERM_MF_FAT	GO:0019209~kinase activator activity	4	0.001663084	16.50
GOTERM_MF_FAT	GO:0019887~protein kinase regulator activity	5	0.007989878	6.29
GOTERM_MF_FAT	GO:0019207~kinase regulator activity	5	0.016550097	5.08
GOTERM_MF_FAT	GO:0008047~enzyme activator activity	7	0.11815578	2.09
Annotation Cluster 9	Enrichment Score: 1.7246819812189633			
Category	Term	Count	*p* value	Fold enrichment
GOTERM_BP_FAT	GO:0007155~cell adhesion	16	0.011769205	2.04
GOTERM_BP_FAT	GO:0022610~biological adhesion	16	0.011947213	2.04
SP_PIR_KEYWORDS	cell adhesion	10	0.047636555	2.12
Annotation Cluster 10	Enrichment Score: 1.5981753824884772			
Category	Term	Count	*p* value	Fold enrichment
SP_PIR_KEYWORDS	cleavage on pair of basic residues	10	0.002927336	3.38
SP_PIR_KEYWORDS	neuropeptide	4	0.005937158	10.72
GOTERM_BP_FAT	GO:0007218~neuropeptide signaling pathway	5	0.023294443	4.58
GOTERM_BP_FAT	GO:0007186~G-protein coupled receptor protein signaling pathway	10	0.999988387	0.38